2Engineering of 3D warp interlock p-aramid fabric structure and its energy absorption capabilities against ballistic impact for body armour applications

Mulat Alubel Abtew, Francois Boussu, Pascal Bruniaux, Carmen Loghin, Irina Cristian

Engineering of 3D warp interlock p-aramid fabric structure and its energy absorption capabilities against ballistic impact for body armour applications

Mulat Alubel ABTEW[1, 2, 3, 4], François BOUSSU[1, 2], Pascal BRUNIAUX[1, 2], Carmen LOGHIN[3] and Irina CRISTIAN[3]

[1]University of Lille 1, Nord de France, France

[2]Ecole Nationale Supérieure des Arts et Industries Textiles (ENSAIT), GEMTEX, 2 allée Louise et Victor Champier, 59056 Roubaix Cedex 1, France

[3]Faculty of Textiles, Leather and Industrial Management, "Gheorghe Asachi" Technical University of Iasi, 53, D. Mangeron Blv., 700050 Iasi, Romania

[4]College of Textile and Clothing Engineering, Soochow University, 178 G.J. D. Road, Suzhou 215021, China

Corresponding author email: mulat-alubel.abtew@ensait.fr or mulat_a@yahoo.com

Abstract: 3D warp interlock fabric became a promising structure to develop women body armour due to its good mouldability. However, its ballistic performance for different threats should be investigated This paper aims to investigate the ballistic performances of 3D interlock p-aramid (Twaron®) fabric panels' against NIJ (National Institute of Justice) standard–0101.06 Level-IIIA. The fabric was manufactured on a semi-automatic loom in GEMTEX Laboratory. 2D plain weave fabric with similar fibre type was also tested for comparison. Various target panels from each structure were arranged and moulded at pre-defined points using an adapted bust-shape forming bench to resemble frontal female body contour. Based on the result, the energy absorption capabilities of 3D interlock and 2D fabric panels with a higher number of layers did not reveal a significant difference. However, the 2D fabric panel absorbed more energy than 3D warp interlock fabrics for a reduced and similar number of layers due to its rigid and stiffness property. Besides, both fabric types had shown less energy transmission to the backing material at the non-moulded target areas as compared to the moulded target area. While shaping the intended panel, 3D interlock fabric revealed better mouldability and less recovery behaviour with less wrinkle formations.

Keywords: 3D warp interlock p-aramid fabric; Ballistic performance; Energy absorption; Women body armour; NIJ-standard; High-performance fibre.

1. INTRODUCTION

Body armour is one of the most important pieces protections of equipment which helps to protect human beings from various critical and fatal injuries [1]. Consequently, many military and law enforcement agencies have made it mandatory for their officers to wear ballistic vests while on duty. This demand not only aggravated the demand of the body armour but also led the progressive improvement of the protection suits by new proper materials constructions [2]. Moreover, the development of high-speed projectiles materials has reconstructed the dynamics of the battlefield which have also advocated the growth of the advanced ballistic protection system not only in terms of better resistance to projectile penetration but also reasonably light in weight, flexible, and comfortable [3]. The ballistic impact is a very complex mechanical process when a low-mass high-velocity impact by a projectile propelled by a source onto a target which mainly effects near the location of impact. The energy absorption before it gains access to the body and energy distribution among the ballistic materials are the two aspects which help to understand the principle and effect of energy transfer from projectile [4]. In body armour systems, different materials from felt to metal and composite, and further bioinspired materials and its biomimetic conditions were used [5]. Moreover, new and innovative materials including fibre, composites, laminates and ceramics have been extensively exploited to accomplish the requirement of a modern military operation, technology-driven war tactics and current terror threats. In general, the effectiveness of the soft body armour related to ballistic impact performance, fitness and comfort depend on the type of ballistic material, material finishing, garment designing techniques, etc. The performance of the ballistic materials toward ballistic impact as a whole depends on not only from individual fibre types [6], but also various combined factors such as boundary conditions, multiple plies and friction [7][8], yarn properties [9], material areal density [10], target plies numbers [11], target ply layering sequence [12][13] and textile construction, such as woven/nonwoven and 2D/3D fabrics [14][15][16] to produce a structural response.

Moreover, Many females personnel's have been joined the law enforcement police and the military services across the world for the last few decades [17]. However, for a long time, they have been exposed to disproportionate protective and functional sacrifices while fitting with male-based pieces of body armour systems. Unlike male, design and manufacturing of female soft body armour encounter problems which need special attention due to its unique curvilinear body shape. Apart from designing techniques, proper material selection and its characteristics also played an important role in the ballistic performances of body armour. Different researchers have investigated the ballistic performances and energy absorptions of different 2D woven material along with different ballistic influential factors for the ballistic armour applications [18][19][20][21][22][23]. Mostly 2D woven fabrics made from high-strength fibres are the most commonly used material in many military and civil applications due to their excellent mechanical properties. The penetration and perforation of targets by projectiles involve highly complex processes which have been investigated experimentally and analytically for the last few decades [13][24][25][26]. For example, the ballistic performance tests of 2D fabric-Twaron CT 710 with various ply numbers and joined with different stitching type were investigated according to NIJ standards for body armour design. The result shows that the fabric ply number and stitching type show significant effects on ballistic properties [27]. One of the inventions also uses around 30 plies of 2D fabrics made of PBO fibre (Zylon®) arranged in a quasi-isotropic orientation to be used for NIJ standard threat Type III-A [28]. Another researcher has developed a novel ballistic protection composite which can provide both cut resistance and impact protection using 40 plies of Kevlar® and Twaron® samples with the areal density of 8202.4gm/m^2 that were glued together with adhesive spray and leather on the top to provide Level IIIA protection [29]. Moreover, apart from 2D fabrics, 3D angle interlock fabric structures also becoming popular and widely used in many technical applications including ballistic applications due to their excellent moulding capability. Various researches have been carried out numerical, analytical and experimental investigations of the ballistic performance of angle-interlock fabrics. Researcher claims 3D warp interlock structures shows not less ballistic protection performance and display good mouldability and lightweight as compared to its counterpart 2D structures [30][31]. For example, one of the researchers investigated the ballistic performance of angle-interlock fabrics to substitute the conventional plain woven fabrics for body armour design and the result clearly showed that angle-interlock fabric is not less than the conventional fabric constructions against ballistic impact. Today, three-dimensional (3D) textiles are enormously involved not only in the ballistic protection but also in various applications [32] due to the enhanced mechanical properties in the thickness direction [33][34], good elastic behaviour properties [35], good formability and mouldability capacity [36] and low shear rigidity as compared to other woven fabric structures [37]. Even though the numerical and analytical studies are mostly limited to 2D woven fabrics, various research works also revealed that 3D textile structures have higher resistance to multi-impacts with the easier and cheaper achievement of complex shape structures in comparison with the 2D fabrics [38]. Another study also tried to define a new 3D woven structure which can compete with 2D stacked fabrics and be a new solution for the ballistic protection in armour vehicles [39]. The ballistic test also confirmed that the fabric meets the required performance and are no less than the conventional fabrics used for ballistic protection [40].

Our previous researches have studied on the design of single and multi-layer pattern generation system for developing seamless female body armour using 3D warp interlock fabrics for better fitness and comfort wear [41][42][43][44]. However, ballistic protection performances are also a very critical parameter that should be considered while developing any kind of body armour. The current research tried to investigate study experimentally mainly the ballistic performances and energy absorptions capabilities of 3D warp interlock and 2D plain fabrics made of 930dTex Twaron® yarn to apply for seamless women soft body protective armour. The ballistic test was carried out both in the non-moulded (f) and moulded (d) surface of the final panel target according to NIJ standard–0101.06 level IIIA [45]. Moreover, the moulding capabilities of the intended fabrics while shaping the body armour panels in order to fit the women body will be also highlighted

2. MATERIAL AND EXPERIMENTAL METHODS

2.1 Material preparation

2.1.1 Ballistic materials

Two different kinds of fabric structures, 3D warp interlock O-L (orthogonal layer by layer) and 2D plain weave, were prepared for ballistic impact performance test against NIJ standard-Level IIIA for women body armour application. The 3D warp interlock fabric made of high-performance p-aramid yarns (Twaron) were design and manufactured in GEMTEX, ENSAIT laboratory using an automatic dobby weaving machine (**Fig. 1**). This fabric structure was designed with the help of TexGen software® as shown in **Fig. 1 (a) and (b**) and drafted using DB weave® software.

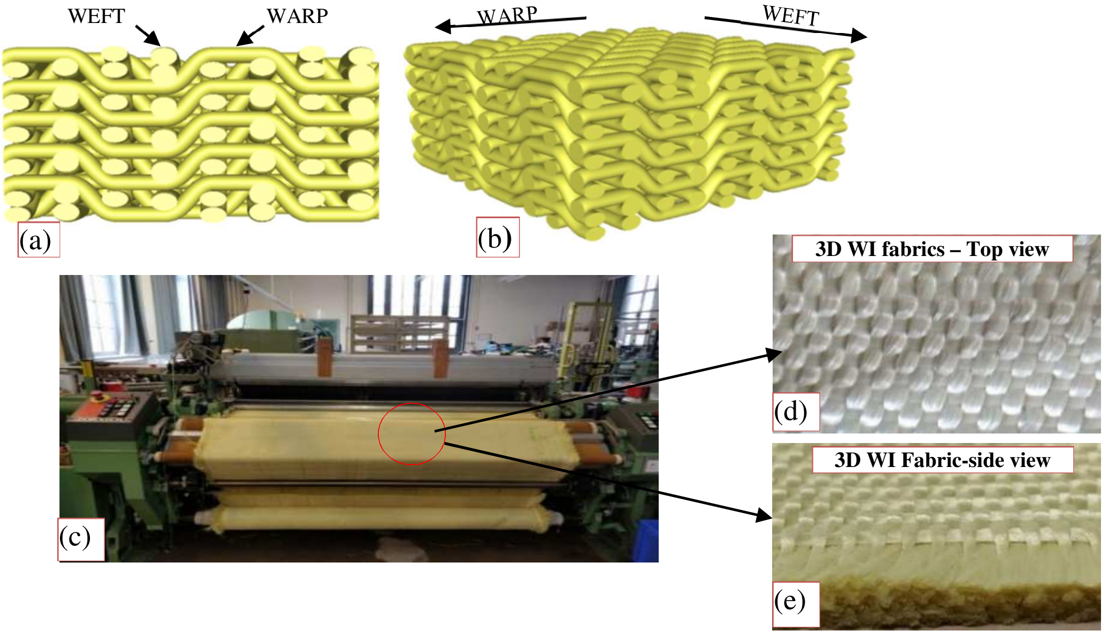

Figure 1 3D warp interlock production process (a) design schematic representation in a cross section (TexGen software); (b) 3D graphical representation (TexGen software); (c) 3D warp interlock fabric production on loom and (d) and (e) Top and side view of the produced 3D warp interlock fabric respectively.

Whereas, 2D plain para-aramid fabric structures (Twaron CT-709) is delivered by Teijin® Aramid Company. Such 2D fabric structure is mainly recommended for women soft body armour manufacturing due to its good ballistic protection performance combined with a high level of mouldability.

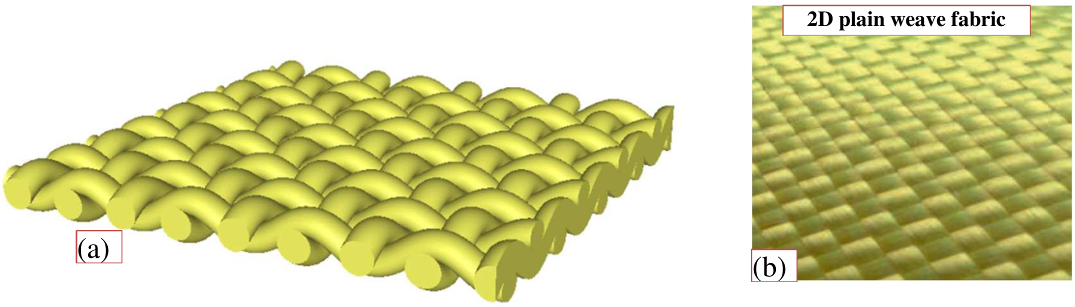

Figure 2 *2D plain weave para-aramid fabric structures, Twaron CT-709 (a) Design schematic representation, and (b) 2D plain weave fabrics*

Table 1 shows the overall specification of 2D plain weave (CT-709) and the 3D warp interlock O-L p-aramid fabric used for this research purpose. The fabric structure of 3D warp interlock O-L and 2D plain weave p-aramid fabrics are shown in **Fig. 1(e) and 2(b)** respectively**.**

__Table 1__ specification of 2D plain(CT-709 fabrics) and 3D O-L warp interlock para-aramid fabrics

Fabric style	No. of weft layers	Linear density [dTex] (Warp/Weft)	Yarn Properties			Fabric Weight [g/m²]	Total Yarn density (Warp/ Weft)/ 10cm	Fabric thickness [mm]
			Tenacity at break [mN/tex]	Breaking force [N]	Elongation at break [%]			
2D plain (CT-709)	1	930(2040 microfilament)	2.35	225	3.45	200	105/105	0.30
3D warp interlock (O-L)	6	930(2040 microfilament)	2.35	225	3.45	1000	525/525	1.55

2.1.2 Target panels preparation

Five different panel targets were established for the specified ballistic test as described in **Table 2**. Among the target, three panels were arranged with 30, 35 and 40 layers of 2D plain weave fabric and the other two panels with 30 and 40 layers of 3D warp interlock fabric layers. All the fabric layers were cut at 500 mm x 500 mm dimensions.

__Table 2__ Panel target description for ballistic performance and energy absorption assessment

Fabric type	Shooting Target System	No of Layers	Total target areal density (g/m²)	Target Weight (g)	Total target thickness(mm)
2D plain weave fabric	S2D-40	40	8000	2000	12
	S2D-35	35	7000	1750	10.5
	S2D-30	30	6000	1500	9
3D warp interlock fabric	S3D-40	40	8000	2000	14.4
	S3D-30	30	6000	1500	10.8

The different layers in the target were prepared in 90/90° arrangement without using any kinds of assembling or stitches. However, each target was taped at its four edges in order to keep the layers at its panel position and prevent unravelling of yarns from the edge.

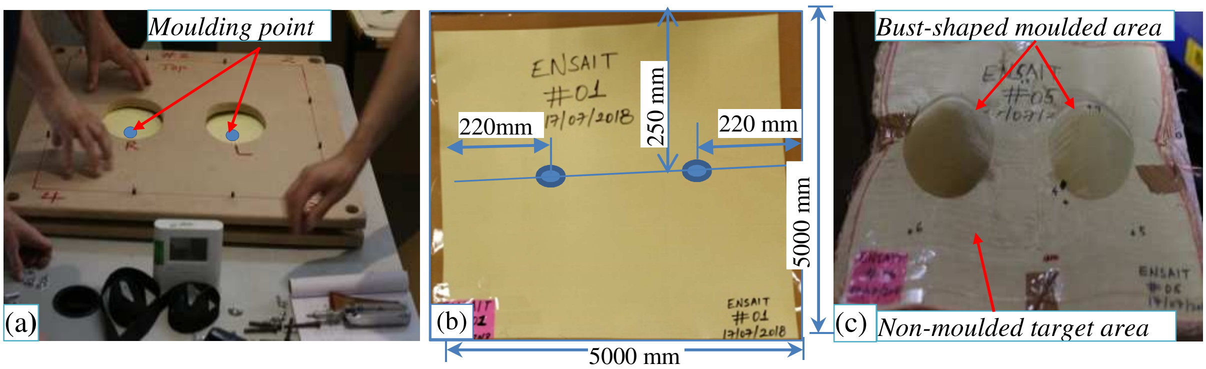

***Figure 3**. Moulded sample target preparation (a) Moulding of target panels on adapted moulding bench, (b) Target panel before moulding, and (d) Moulded sample target panel.*

The targets were kept in the black plastic bags to protect the fabric from the environmental effects. Before the ballistic test, each target panels were moulded at two pre-defined bust points to resemble the women body shape of 90B bust size. The moulding process was carried out using an adapted punching bench with a bust-shaped moulded punch as shown in **Fig. 3.**

2.2 Experimental Methods

2.2.1 Ballistic test equipment

The test apparatus which is adapted to NIJ 0101.06 Standard Level-IIIA [46] was used for the ballistic performance investigation as shown in **Fig. 5 (a).** Such Standard level would give the highest level of ballistic protection among the soft body armour category. The distance between the firing gun barrel of the testing apparatus and the panel target was measured 10 meters. Moreover, the exiting projectile velocity measuring unit (Radar Doppler) was positioned at the mid position (5 m) between the firing gun barrel and the target panels. The chronograph was also placed at 9 m from testing devise for detecting and measuring the impact speed of the projectile through the photoelectric principle. MP5 gun with bullet core weight of 8 g (124 gr) and 9 mm diameter as shown in **Fig. 4 (b)** was used in the ballistic shootings test. All the bullets were provided by CREL (Centre de Recherche et D'Expertise De La Logistique of France), where tests were carried out.

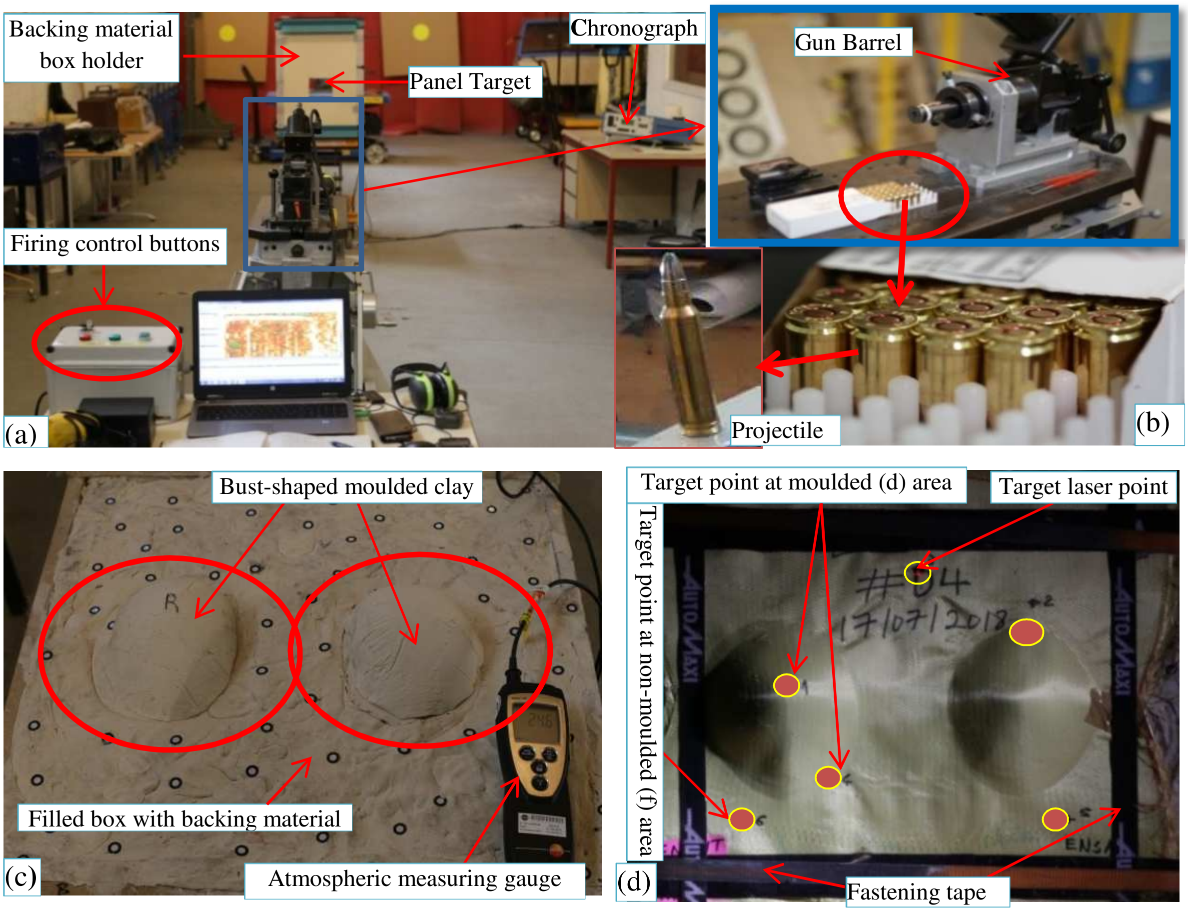

Figure 4 *Ballistic testing set-up and backing material (a) Ballistic test apparatus, (b) gun barrel and bullet used, (c) Square box filled with backing clay material and bust-shaped moulded clay, and (d) panel target with shooting point*

According to the NIJ Standards, Roma Plastilina # 1 moulding clay was used as the backing material due to it is cheap, readily available, and attained higher deformation with time compare to other backing material[47]. This moulding clay material was then properly filled in a target panel supporting square box made with wood material. The volume of moulding clay inside this box measures 50 cm tall, 50 cm wide and 10 cm deep. The bust-shaped model from the same moulding clay was also prepared to fit the moulded target area as shown in **Fig. 4 (c)**. The hardness of moulding clay was calibrated before each test using a half sphere tip iron with 1kg weight and 45 mm diameter. This calibration would later help to compute the energy absorbed by each panel target during the ballistic impact.

2.2.2 Ballistic shooting test and procedures

The SMG (Sub Sterling Gun) gun system used standard 9 x19 mm Full Metal Jacketed Round Nose (FMJ RN) bullets to fire at velocities of 426 ± 9 m/s. The moulded panel target was carefully affixed to the front of the moulding clay filled supporting square box with adjustable elastic straps at the edges as shown in **Fig. 5 (c).** The moulding clay allows us later to measure the intended backface signature at the back for every shot**.** The ballistic impact test for all panel target was performed in an indoor ballistic shooting compound with defined and standard atmospheric conditions (T°=24.1°C HR=53%). For each panel target, three shots (shot 1, 2 and 4) on the moulded (d) area and another three shots (shot 3, 5 and 6) on the non-moulded (f) area of the panels was targeted according to the NIJ standard **Fig. 5 (d).** After every panel shots, the trauma indentation created on the backing material were computed using handy scanning device as described in **section 2.2.3**. The firing system was controlled automatically and guided by the laser pointer which helps to precisely shoot on the intended target point.

2.2.3 Back Face Signature (BFS) or Blunt Trauma modelling and its measurement

The back face signatures after each test shall be precisely measured and analyzed to determine not only whether the intended armour panels will provide adequate protection against the projectile but also to compute the energy absorbed by each panel. The following sections will explain how to measure the back face signatures from each P-BFS test of the intended different panel target to determine their respective energy absorption capabilities.

2.2.3.1 Back face signature (BFS) modelling

Back face signature is one of the most important parameters which help to determine the impact energy exerted in the panel during the ballistic test. The depth, diameter and volume of blunt trauma are formed at the backing material if only the shooting bullet did not pass through the panel target. The values of those parameters will indicate how the bullet kinetic energy with the specified velocity is absorbed by the panel target and transmitted to the backing materials. In this study, the blunt trauma indentation in the form of moulded shape was obtained by scanning the deformed surface of backing material after each panel target test as shown in **Fig. 6.** A very precise handy scanning device (**Fig. 5 (d)**) was employed to capture the whole backing material surface without any physical contact for further computing blunt trauma volumes. Computing such trauma volume from scanned geometry for each shot helps to determine the amount of energy absorbed by each target panels. Before scanning, the target along with backing material box (**Fig. 5 (b)**) was detached from the fixed ballistic box holder, and then the target will be removed carefully from the backing material.

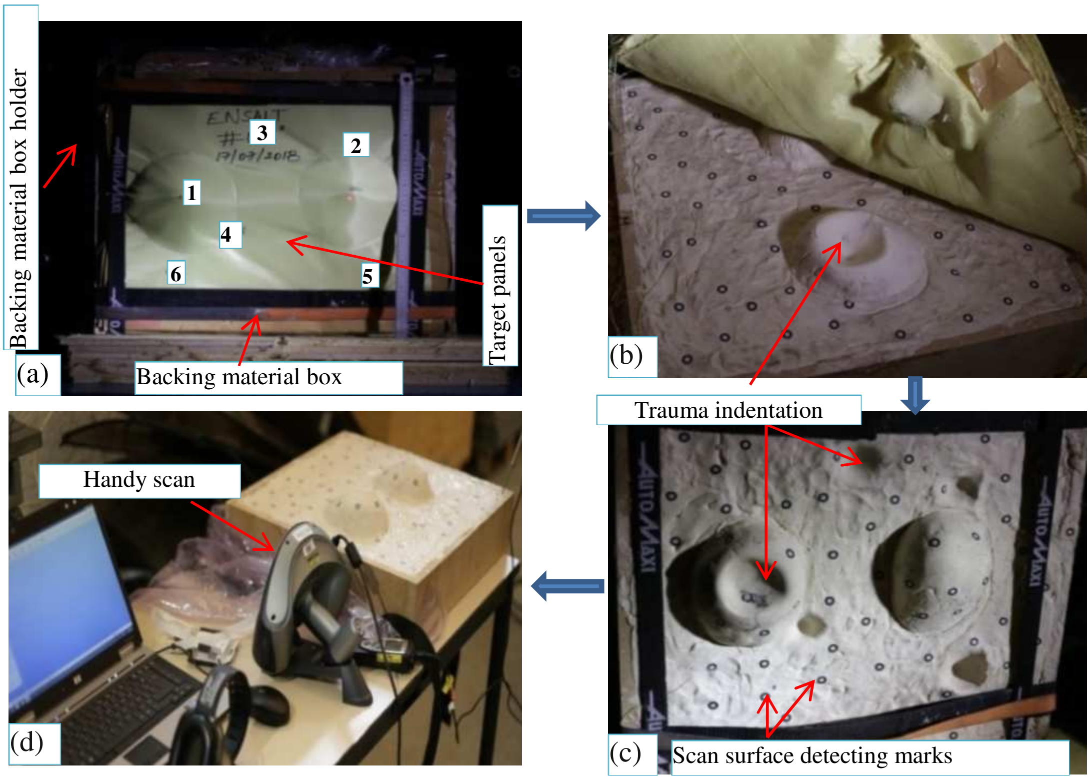

Figure 5 *Blunt trauma measurement process (a) Panels for the ballistic test (b) Blunt trauma indentation after shooting, (c) All the trauma indentation and, ((d) Scanning of backing material after the test using the handy scanner for trauma measurement.*

This would help not only to keep the tested target but also not to distort the trauma volume created on the surfaces of the backing material. While scanning, different reflecting marks were placed on the deformed backing material surface for easy detection and modelling of the trauma deformation ((**Fig. 5 (c)**). The tested backing surface was scanned at a time after each target shot for better scanning process and time-consuming purpose. Such scanning methods not only give a precise result and measurement in a short time but also make it easy to compare visually the trauma for different panel target.

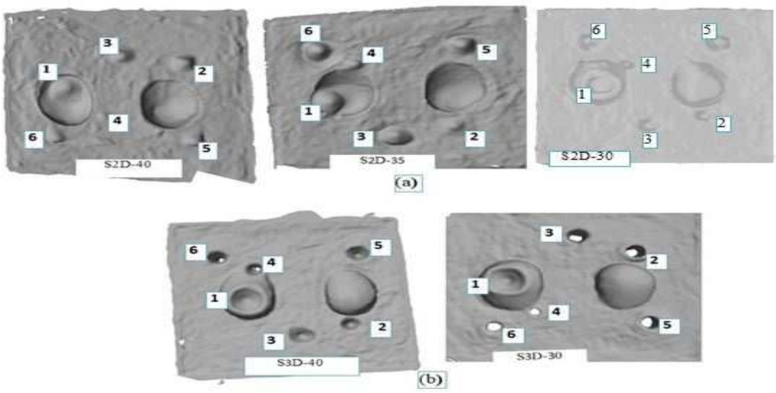

Figure 6 *Scanned backing material after ballistic test and its trauma indentations of different panel targets (a) 2D plain weave and (b) 3D warp interlock fabrics.*

2.2.3.2 Blunt trauma volume determination

The energy absorption capacities of the targets were mainly computed based on the backing material trauma volume. Thus, modelling the exact blunt trauma volume of each target for every shot is very crucial. The scanned 3D trauma surface by the handy scanner as shown in **Fig. 6** was transferred to the 3D CAD modelling software (3D design concept) to model and measure the exact volumes of target trauma as shown in **Fig. 7**. While modelling, first, the inner and outer trauma contour frame-line (as shown in **Fig. 7 (b)**) was conceded following the exact trauma surface to map the shell of the trauma. Then, the outer and inner surface meshes were developed based on the trauma shell, and stitched together to develop the exact trauma volume as illustrated in **Fig. 7 (c) and (d).**

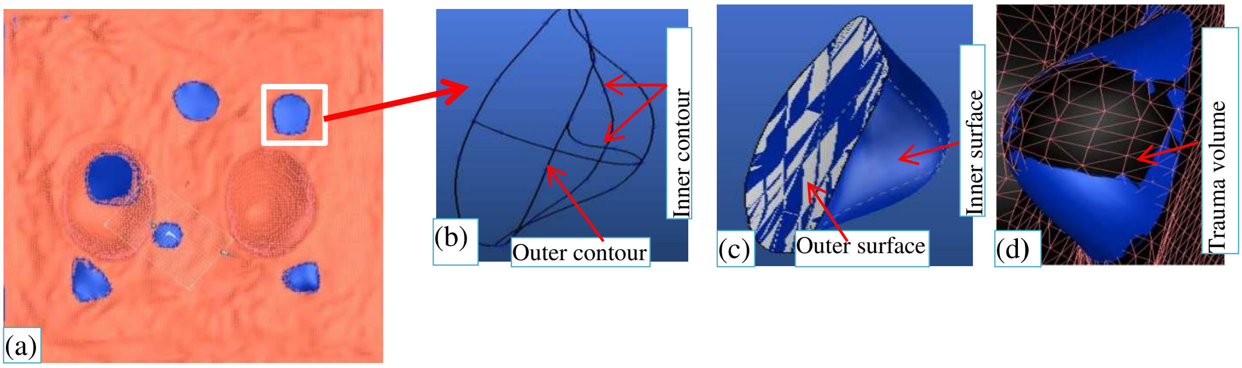

Figure 7 *Determinations of trauma volumes for different target shot using 3D design software (a) Modelled 3D backing material surface with different shot trauma (b) Creation of internal and outer framework following the trauma indentation (c) Modelling of out and inner surface mesh trauma volume (d) Stitched out and inner surface to develop blunt trauma volume.*

2.2.4 Backing material, energy absorption and its calibrations

The moulding clay trauma indentations have been calibrated before the actual ballistic testing to determine the exact absorbed energy by each target. This calibration further helps not only keeps consistency throughout the test but also helps to compute the energy exerted on a unit volume of trauma (J/mm^3) in the moulding clay material. During the calibration process, a cylindrical shape and semi-spherical tipped iron bar weighing 1 Kg and 60 mm diameter were dropped properly on drop point of conditioned backing material from 2.0 m height through the confined hollow tubes based on NIJ standard [46] as shown in **Fig. 8.** After each drop test, the trauma volumes were scanned and measured with precision. The arithmetic average values of five drop test trauma volumes were recorded for further analysis. Its average trauma depth and volume values were recorded 22 mm and 23 mm^3 respectively. These arithmetic numbers are approximately found similar to the values recommended by NIJ 0101.06 standards at 2 m height (19 mm ± 2 mm).

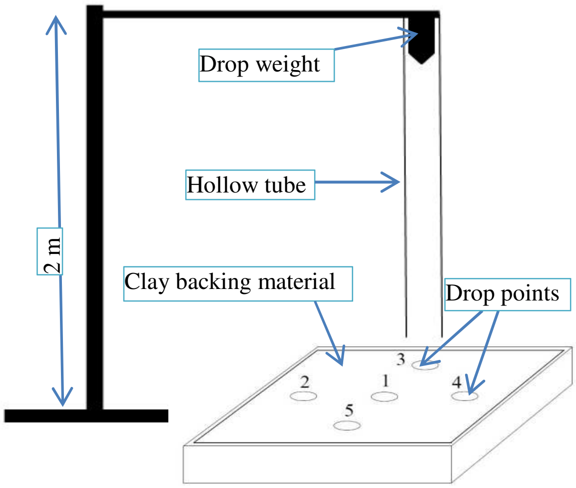

Figure 8 *Calibrations of clay backing material.*

Base on this average volumes of the trauma at the mentioned height (2 m), it is now possible to calculate the unit trauma energies ((E_{volume}) (J/mm^3) by the moulding clay material as shown in **Table 3**. This unit trauma potential energy of the dropped weight ($EP_{measured}$) was calculated using the following classical formula:

$$EP_{measured} = m \cdot g \cdot h \quad [J] \qquad (1)$$

Where:
m - is the weight of the semi-spherical tipped iron bar [kg];
g - the gravitational acceleration [m/s^2];
h - the dropping height [m].

Table 3. *Average unit trauma energy determinations from the drop test*

Height (m)	Drop test	BFS (mm)	Trauma volume (mm^3)	$EP_{measured}$ (J)	$E_{unit\ volume}$ (J/mm^3)	$E_{ave\ unit\ volume}$ (J/mm^3)
2	Test 1	24.1	24.665	19.62	7.95×10^{-4}	**8.3×10^{-4}**
	Test 2	23.5	23.599	19.62	8.31×10^{-4}	
	Test 3	20.15	22.756	19.62	8.62×10^{-4}	
	Test 4	21.22	22.158	19.62	8.85×10^{-4}	
	Test 5	22.11	25.164	19.62	7.8×10^{-4}	
	Average	**22.24**	**23.665**	**19.62**	**8.3×10^{-4}**	

The unit volume energy of each drop test ($E_{unit\ volume}$) was calculated using the following formula:

$$E_{unit\ volume} = \frac{EP_{measured}}{V_{trauma\ calculate}} \quad [J/mm^3] \qquad (2)$$

Where:
$EP_{measured}$ -is the calculated potential energy by the drop weight for each test [J];
$V_{trauma\ calculate}$ - the volume of the trauma formed by weight dropped on backing material [mm^3].

Determination of the average trauma volume ($V_{average\ trauma\ calculate}$ (23.665mm^3)), on the backing material helps to compute the average unit potential energy ($E_{ave\ volume}$). According to the test result and shown in **Table 3**, the average unit volume energy ($E_{ave\ unit\ volume}$) were found 8.3×10^{-4} J/mm^3. Based on this computed value, it is now possible to calculate and correlate the values with the energy absorbed and transmitted by the panel target while ballistic shooting. The energy absorbed by the ballistic test ($E_{ballistic}$) mainly depends on the trauma volume for every target test and calculated as follows:

$$E_{ballistic} = V_{trauma\ ballistic} \cdot E_{ave\ unit\ volume} \qquad (3)$$

Where:

$V_{ballistic}$ - is the trauma volume created while ballistic test;

$E_{ave\ volume}$ - the potential energy developed by the trauma volume during dropping test.

Moreover, the kinetic energy of the ballistic bullet just before it touches the fabric panel target ($EK_{ballistic}$ - is computed as follows:

$$EK_{ballistic} = \frac{m \cdot v^2}{2} \quad [J] \qquad (4)$$

Where:

m - is the mass of the bullet [kg];

v - the speed of the bullet [m/s].

During the ballistic test, the target tried to prevent the bullet from penetration through different mechanisms. However, some portion of kinetic energy will be absorbed by target and the rest passes beyond the target to generate an indentation on the backing materials. Computing such absorbed and transmitted energy values would help to compare the performance of different fabric panel target during ballistic impact tests. Thus, it is now possible to compute the energy absorbed by the target panels ($Ea_{ballistic}$) considering both the calculated kinetic energy ($EK_{ballistic}$) and the amount of energy transmitted ($Et_{ballistic}$) to the backing material

$$Ea_{ballistic} = Ek_{ballistic} - Et_{ballistic} \qquad (5)$$

Where:

$Ek_{ballistic}$ is the energy from kinetic energy of the bullet;

$Et_{ballistic}$ - the energy transmitted beyond the panel target and exerted on the backing materials.

3. RESULTS AND DISCUSSION

In the non-perforation case of ballistic test, the values of trauma indentations for the different target panels were measured and analyzed. The trauma volume could mainly help to determine the energy transmitted to the back of a panel. For instance, the smaller the trauma volume at the backing material would indicates the energy was propagated in the larger part of the panels and only smaller amount of energy was transmitted to the back of the materials and vice versa.

Table 4. *Impact projectile velocity, energy absorbed by fabric layers and energy transmitted to the back of the panels of different panel layers of 2D plain weave and 3D warp interlock p-aramid fabrics*

Fabric Type	No. of layers	Designations	Shot No.	Impact bullet velocity (m/s)	Kinetic (Impact) Energy (J)	Trauma Volume (mm^3)	Energy transmitted (J)	Energy absorbed by the panel, Ea (J)
2D plain Plain weave	30	2D-30	1	404.0	652.9	43498	36.1	616.8
			2	407.3	663.6	39764	33.0	630.6
			3	402.8	649.0	18881	15.7	633.32
			4	409.4	670.4	34440	28.6	641.9
			5	404.4	654.2	8583	7.1	647.0
			6	408.2	666.5	15786	13.1	653.4
	35	2D-35	1	406.5	661.0	39764	33.0	628.0
			2	402.7	648.7	36175	30.0	618.6
			3	409.3	670.1	14673	12.2	658.0
			4	412.9	682.0	24786	20.6	661.4
			5	411.4	677.0	6060	5.0	672.0
			6	410.2	673.1	11231	9.3	663.7
	40	2D-40	1	408.1	665.9	24593	20.4	645.5
			2	408.2	666.5	18123	15.0	651.5
			3	404.7	655.1	6797	5.6	649.5
			4	409.4	670.4	18067	15	655.4
			5	408.7	668.1	7797	6.5	661.7
			6	405.0	656.1	2159	1.8	654.3
3D warp interlock (O-L)	30	3D-30	1	404.0	669.1	54,136	45.0	624.1
			2	407.3	684.9	-	-	684.9
			3	402.8	671.1	-	-	671.1
			4	409.4	690.6	-	-	690.6
			5	404.5	665.2	-	-	665.2
			6	408.2	674.0	-	-	674.0
	40	3D-40	1	410.4	673.7	40742	33.8	639.9
			2	410.1	672.0	37574	15.2	656.8
			3	400.2	640.6	16236	13.5	627.2
			4	414.3	686.6	20547	17.1	669.6
			5	413.3	682.3	3794	3.2	679.1
			6	409.6	671.2	10589	8.8	662.4

3.1 Energy absorption capability of 3D and 2D p-aramid fabric panels

In general, when the fabric panel is impacted by the high-speed bullet, the energy exerted by the projectile will be converted mainly into kinetic energy. Some portion of this kinetic energy are absorbed by each layer of the panels whereas, the remaining portions will be transmitted to the back of the target to create indentation on the backing materials. The amount of energy absorbed by the target mainly depends on various internal and external ballistic performance factors. While ballistic impact, the energy generates a shock wave propagations on the fabrics surface which in turn damages the filaments, fibres, and yarns. The energy might also ultimately causes distortion of the fabric layer in the longitudinal direction. Investigating the energy absorbed by the target panels and the transmitted energy to the backing material would help to understand such ballistic impact phenomenon.

In our current investigations, both target panels made of 3D warp interlock O-L and 2D plain weave fabric undergo to deformation to resist the propagating energy exerted by the projectiles. **Table 4** shows the different projectile impact velocity, impact energy, and target panels with their corresponding absorbed and transmitted energy. The kinetic energy generated on the target might be different from one to another shot due to the projectile speed difference even using same projectile mass throughout the test.

The following sub-section will discuss on the energy absorption by the different panels of 2D and 3D warp interlock O-L fabrics based on the shooting target, target areas (deformed and flat) and type of fabric structures (2D and 3D fabrics) with nearly similar fabric layers and panel areal densities.

3.1.1 Effect of shooting points on energy absorption capabilities of targets

The kinetic energy of a bullet is the energy applied and affecting the panel targets during ballistic impact tests. Such kinetic energy generated by the projectile on the target panels mainly depends on the projectile speed considering other factors constant including the mass of the bullet throughout the test. This energy should be absorbed fully absorbed at least by the final panel target before perforation and created some damages on the vital organs of the human body. Besides, the energy absorption capabilities of the panel target will be affected by different influential parameters. Material properties, type of fabric structure, layers arrangement and it' finishing on the panels, panel thickness (areal density) and projectile geometries are some of the main parameters. In this section, the energy absorption capabilities of targets made of 3D warp interlock and 2D plain weave fabrics with different target systems and target point conditions (moulded and non-moulded) will be enlightened. **Fig. 9 (a) and (b)** shows the absorbed and transmitted energies and their percentage (%) values respectively for 40 layers of 2D plain p-aramid fabric at moulded (d) and non-moulded (f) shooting points.

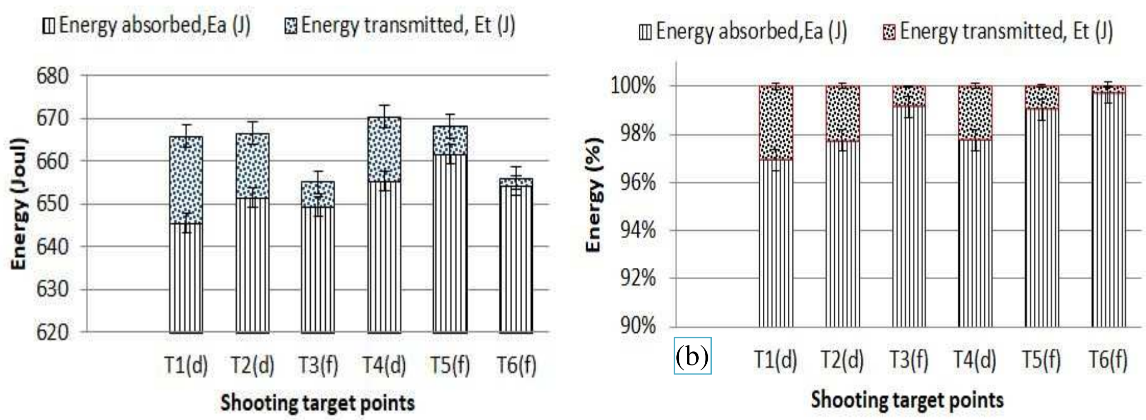

Figure 9 *Ballistic results of 40 layers of 2D plain weave fabric at different shooting areas (moulded (d) and non-moulded (f) area) (b) Values of absorbed and transmitted energy in Joule and (b) Percentages (%) of absorbed and transmitted energy.*

As indicated in **Fig. 9 (a)**, the total energy exerted on deformed (d) target areas T1 (d), T2 (d) and T4 (d) shows higher values as compared to non-moulded (f) target area, T3(f) and T6(f). However, the initial total impact energy does not indicate how much energy is absorbed by the intended panel and transmitted to the backing material of that particular target area. Based on the trauma volume-energy computation, the transmitted energies for T1 (d), T2 (d), T3 (f), T4 (d), T5 (f) and T6 (f) were found to be 20.4, 15.04, 5.64, 14.99, 6.47 and 1.79 J respectively. For better comparison, it is also important to compute the percentage values of energy absorbed by each target points with respect to the total of impact energy exerted on the respective target area. **Fig. 9 (b)** shows the percentage (%) of energy absorbed and transmitted by 40 layers of 2D plain weave p-aramid panel with shot points. Based on the result, a significant difference in energy absorbed and transmitted by the panel was found among the non-moulded (f) and moulded (d) target points. The moulded (d) target points (T1 (d), T2 (d) and T4 (d)) shows a higher percentage of energy transmitted as compared to non-moulded (f) target points(T3 (d) and T6 (f)). For example, the absorbed energy percentages of T1 (d), T2 (d) and T4 (d) recorded as 96.93%, 97.74%, and 97.76%, whereas for T3 (f), T5 (f) and T6 (f) are 99.14%, 99.03% and 99.73%. This lower energy absorbing capabilities of the moulded area of 2D fabric panel might arise from various moulding defects which could hinder the ballistic protection performances of those particular areas.

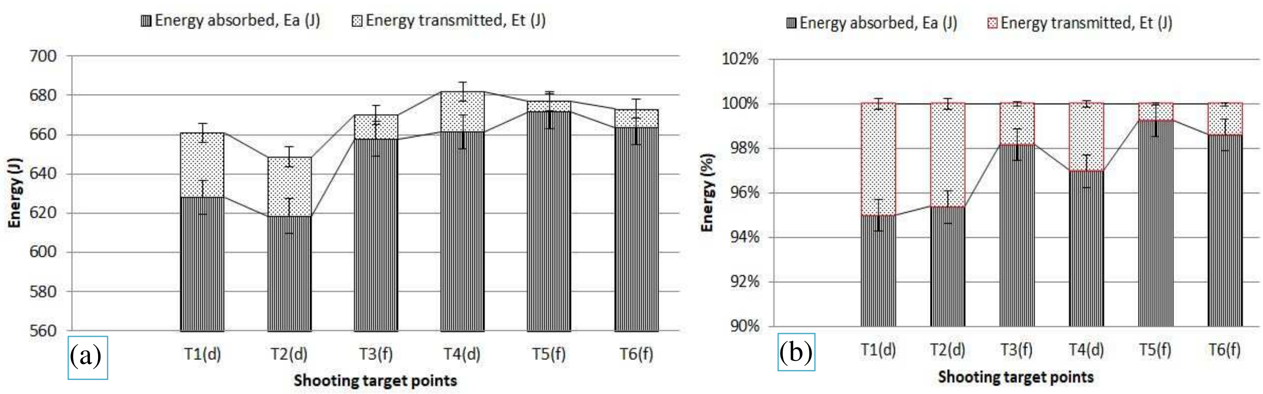

***Figure 10** Ballistic results of 35 layers of 2D plain weave fabric at different shooting areas (moulded (d) and non-moulded (f) area) (a) Values of absorbed and transmitted energy in Joule and (b) Percentages (%) of absorbed and transmitted energy.*

The absorbed and transmitted energy values and their percentage (%) of the target made with 35 layers of 2D fabric at different shooting points are also shown in **Fig. 10 (a) and (b)** respectively. Based on these observations, the target energy transmitted values at the moulded area shows higher values than the non-moulded areas. For example, target points T1 (d), T2 (d), T3 (f), T4 (d), T5 (f) and T6 (f) recorded 33, 30, 12.18, 20.57, 5.03 and 9.32 J values of transmitting energy values. Similarly, targets at the moulded areas revealed much higher energy transmitted percentage than the non-moulded target areas. The energy transmitted percentage beyond the panels at shots target area T1 (d), T2 (d), T4(d) are 4.99% , 4.63% and 3.02%, whereas shots at the target areas T3 (f), T5 (f) and T6 (f) were recorded 1.8%, 0.74%, 1.38%. In general, it was found 4.25% value differences in the transmitted energy between the highest value (4.99%) at T1 (d) and lowest value (0.74%) of T5 (f). Different energy transmitted percentage values were also observed at different target points within the same target panel). For example, the energy transmitted percentage of the target with 35 2D fabrics layers shows 3.19% and 2.28% difference between the highest (T1 (d) & T3 (f)) and the lowest (T4(d) & T5 (f)) target points.

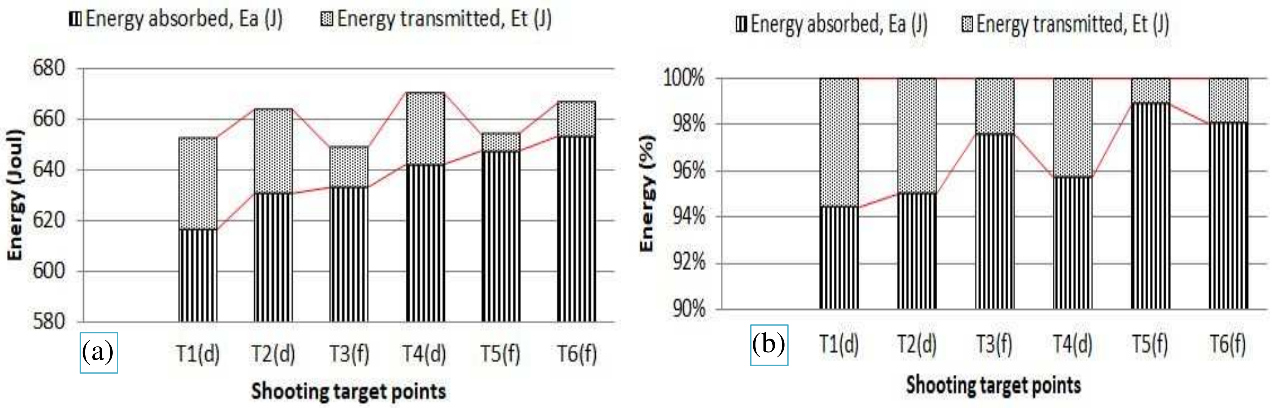

Figure 11 *Ballistic results of 30 layers of 2D plain fabric at different shooting areas (moulded (d) and non-moulded (f)) (a) Values of absorbed and transmitted energy in Joule and (b) Percentages (%) of absorbed and transmitted energy.*

Similarly, the energy absorption and transmitted values for 30 layers of 2D plain fabric at different shooting areas show a similar trend as discussed in the previous target panels. Its energy absorption and transmitted values are shown in **Fig. 11 (a) and (b)**. The energy percentage of absorbed by moulded (d) target area of T1 (d), T2 (d) and T4 (d) were recorded as 94.45%, 95.03% and 95.74%. Whereas, percentage of the energy absorbed for non-moulded (f) target points T3 (f), T5 (f) and T6 (f) show 97.58%, 98.9% and 98.03%. The panel has also revealed maximum and minimum energy absorption percentage capabilities in target points of T5 (f) (non-moulded (f)) and target points of T1 (d) (moulded (d) respectively Moreover, the energy absorption capabilities of the 30 layer panels shows smaller values as compared to the 35 and 40 layers both in the moulded (d) and non-moulded (f) target points. In general, the result indicated that the energy absorbed by the panel and transmitted energy was affected by the number of fabric layers and specific target point conditions.

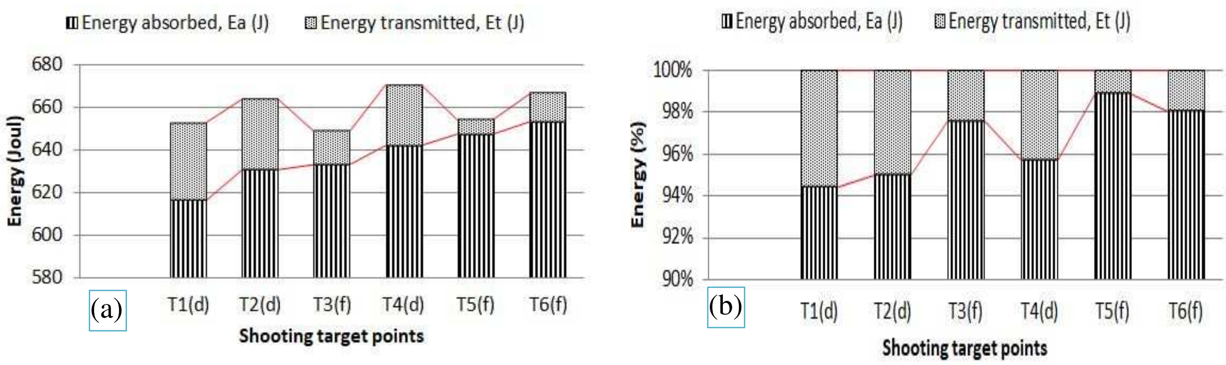

Figure 12 *Ballistic results of 40 layers of 3D warp interlock fabric at different shooting areas (moulded (f) and non-moulded (f) area) (a) Values of absorbed and transmitted energy in Joule and (b) Percentages (%) of absorbed and transmitted energy*

The energy absorption and transmitted capabilities and its percentage (%) of 3D warp interlock fabric with different layers at the moulded and non-moulded target areas were also examined. **Fig. 12 (a) and (b)** shows the absorbed and transmitted energy values of different target points and their percentages (%) of target panels made with 40 layers of 3D warp interlock fabric. Different impact energy was generated at different target points of panels made with 3D warp interlocks fabrics. This is mainly due to the different impact bullet velocity exerted at the respective target points. Owing to such circumstance, it is not possible solely to compare the energy absorption capabilities of each target areas using numerical energy (Joule) values. For instance, the total impact energy exerted and energy absorbed by the panels at target points T1 (d), T2 (d), T3 (f), T4 (d), T5 (f) and T6 (f) were found 639.88, 656.78, 627.16, 669.53, 679.12 and 662.43 J respectively.

However, the percentages of energy absorption of T 1(d), T2 (d), T3 (f), T4 (d), T5 (f) and T6 (f) were recorded as 94.98%, 97.74%, 97.89%, 97.51%, 99.54% and 98.69% respectively. This clearly indicated that energy percentage values will give a better room for comparisons of different target points within the same target than specific energy values (J). Unlike 2D fabric panel targets, the energy absorbed and transmitted values of 3D warp interlock fabric exhibit differently. For example, except the two extreme higher (99.54%) and lower (94.98%) percentage values at target point T5 (f) and T1 (d) respectively, other target points did not show as such significant difference. Target point T1(d), T2(d), T3(f), T4(d), T5(f), and T6(f) of target panels with 40 layers of 3D warp interlock fabrics possess 5.02%, 2.26%, 2.1%, 2.48%, 0.46% and 1.31% of energy transmitted values. In fact, the increase in the transmitted energy almost corresponds to the decrease in the absorbed energy. The moulding process did not also significantly affected by the ballistic performances of 3D fabric panel while shaping the panel in order to make the intended target form.

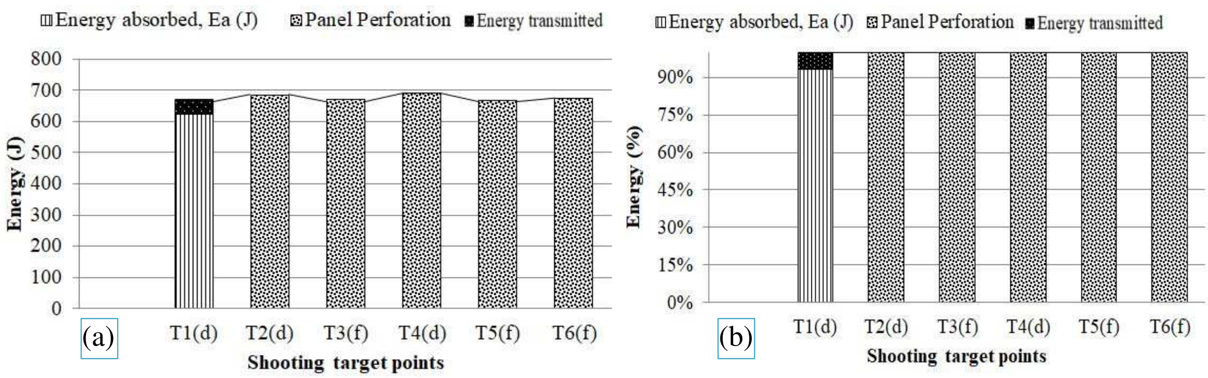

Figure 13 *Ballistic results of 30 layers of 3D warp interlock fabric at different shooting areas (moulded (d) and non-moulded (f) area) (a) Values of absorbed and transmitted energy in Joule and (b) Percentages (%) of absorbed and transmitted energy.*

Moreover, **Fig.13 (a) and (b)** shows the energy absorbed and percentage (%) values of panels made with 30 layers of 3D warp interlock fabric at different moulded (d) and non-moulded (f) points. The energy absorbed by the panel was calculated only when the panel is not penetrated. In this panel target, except for T1 (d), all the target points were unable to resist the ballistic impact from penetration and not considered for further analysis. The energy transmitted percentage in T1 (d) for panels made with 30 and 40 layers of 3D warp interlock fabrics were recorded as 93.28% and 94.98%. The number of layer involved in the panels made with both 2D and 3D warp interlock fabrics were affected and contributed for energy absorption capacities. Moreover, the panel target point conditions (moulded and non-moulded) were also more or less affected the energy absorbing capabilities of both 2D plain fabrics panels. However, only limited outcomes on the energy absorption and transmitted values were observed in the moulded target points of the panel made with 3D warp fabric layers. This indicates that shots on moulded (d) and non-moulded (f) target areas of 3D warp interlock fabrics shows nearly similar energy absorbed percentages as compared to its counterpart 2D plain weave fabrics at similar target areas and fabric density. This is due to the fact that a 3D warp interlock fabric shows good mouldability without affecting the mechanical performances of the final products. The panel rigidity could also increase with the compactness of the respected fabric type. Such behavior in turn brings a positive upshot on the energy absorbing performances of the target.

3.1.2 Comparisons of energy absorption capabilities 2D plain and 3D warp interlock fabrics panels at different shot points

During the design of ballistic protection panel, its weight should be taken into consideration as much as ballistic performance is considered. The number of fabric layers (ply) in the target panel system has a direct relation to its energy absorbing capabilities. The more the fabric layers in the panel system, the higher the energy will be absorbed by panels and the lesser energy transmitted to the back of the panel. However, as the number of fabric ply in the panel increases, the flexibility of the ballistic panel could be decrease and panel might become more rigidity. This contradiction makes it very difficult to achieve the body armour entailing both light weighted wears along with better ballistic protection performance. Rigid ballistic panels also not only limit the movement ability of the user but also create difficulty in the design and production process of body armour. Considering this, different ballistic material which encompasses the above parameter was investigated for optimization of the final products. In this situation, both trauma indentation, energy absorption and other parameters should be optimized by considering body armour rigidity and weight. This section will thoroughly discuss the energy absorption capabilities of panels composing different layers of 2D plain weave and 3D warp interlock fabric layers. **Fig. 14** shows the average energy absorption and transmission values (joule) and its percentage (%) of 2D fabric with different layers at non-moulded (f) area. Based on that result, the energy absorption capacity of the panel significantly increased as the number of ply fabric increases.

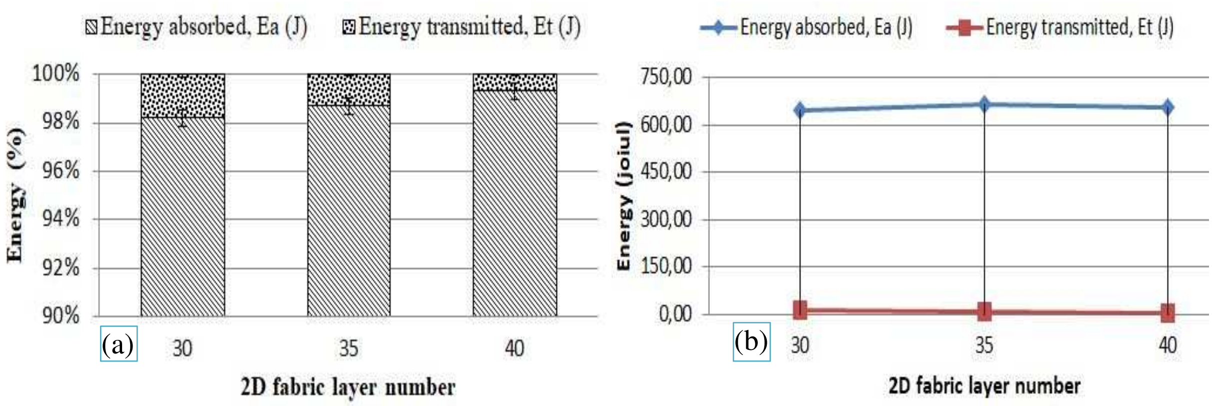

Figure 14 *Average energy absorption and transmission and its percentage of 2D fabric with different layers at non-moulded (f) area (shot 3, 5 and 6).*

The average energy transmitted to the back of the panel in the non-moulded target points was also recorded as 11.97 J, 8.84 J and 4.63 J for 30, 35 and 40-plies of 2D plain weave fabric respectively. Whereas, the average percentages (%) of energy transmitted by panels made with 30, 35 and 40-layers of 2D fabric were also computed as 1.82%, 1.31% and 0.70% at the non-moulded shot points. This clearly shows that panels made with 40-plies 2D fabrics transmitted 1.11% and 0.6% less energy values as compared to panels with 30 and 35-layers of 2D fabrics respectively. Besides, the result also clearly shows the energy absorbed has been increasing when the layers have been increased from 30 to 35 and 35 to 40. **Fig. 15** also shown the average energy absorption and its percentage of panels made with different layers of 2D fabric at moulded (d) points. The average energy absorption by the panel and transmitted to the back of the panel is 629.72J, 636J, 650.79J and 32.56J, 27.87J, 16.82J for 30, 35 and 40-plies of 2D fabric respectively. Moreover, at the moulded (d) target points, the panel with 30, 35 and 40-plies of 2D fabric absorbs average percentage (%) of 95.08%, 95.8% and 97.48% of the total projectile kinetic energy. This indicated that 40-plies of 2D fabric has also absorbed an average 2.4% more energy as compare to 30-layers of 2D fabric at the moulded (d) target points. However, 35-plies of 2D fabric absorb almost equal average energy as compared to 30-layers of 2D fabric. This clearly shows that as the number of layers in the panel increases, the energy absorption capabilities of the target made of 3D warp interlock and 2D plain weave fabric become insignificant.

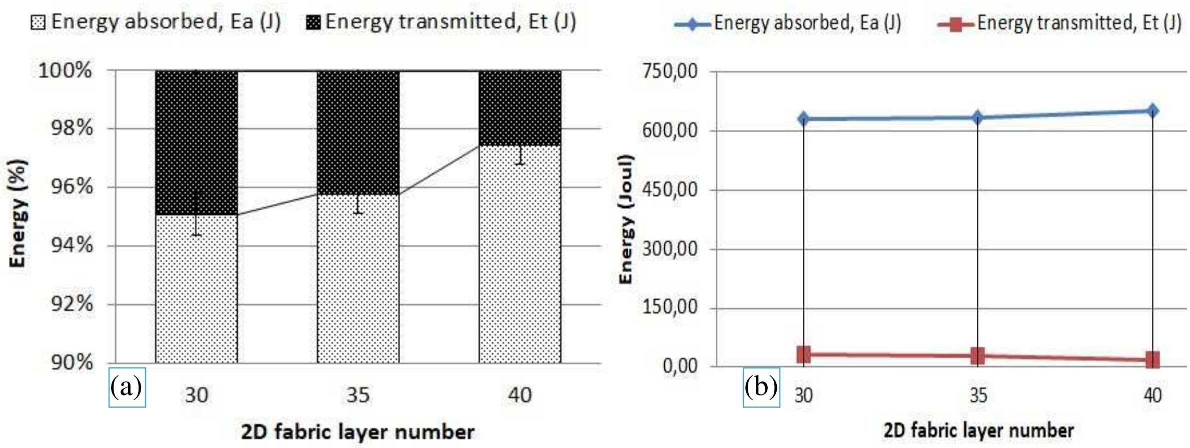

Figure 15 *Average energy absorption and transmission and its percentage of 2D fabric with different layers at moulded (d) area (shot 1, 2 and 4).*

3.1.3 Effect of fabric structure on energy absorption capabilities at different target areas

Nowadays high-strength woven fabrics made of polymeric yarns are widely used for the ballistic materials due to their low density and high toughness. This material will also give good resistance to high-speed loading, particularly during ballistic impact. Though, their response to impact is complex because of the final material fabric architecture, target conditions and rate-dependent behaviour of their constituent yarns. Different researches have been studied on the different influential factors of the ballistic performances of materials. Among the different parameters, fabric construction was found one of the key factors affecting the performance of ballistic fabrics.

This section tried to presents the influence of fabric structures (2D plain weave and 3D warp interlock fabrics) on the ballistic impact performances and energy absorption capabilities of the final target. Moreover, the comparison has been also considered not only the type of fabric structure but also the impact point condition (moulded (d) and non-moulded (f)) of the fabric panels. **Fig. 16** illustrated the average energy absorption by the panel and transmitted to the backing material of percentage (%) values of 2D plain weave and 3D warp interlock fabrics. For a better analysis, the same numbers of layers (40 layers) with similar fabric densities for both fabric structures at similar target points were considered. The energy absorbed by the moulded (d) target panel of 2D plain and 3D warp interlock p-aramid fabric panels were found 650.79J and 655.4J. Whereas its energy transmitted energy to the backing material are recorded with 16.82J and 22.03J. However, due to the different initial impact energy which emanates from impact projectile velocity, the energy absorbed and transmitted energy values might be different. Considering this it is necessary and efficient to analyses the intended panel energy absorption capabilities in terms of fraction or percentages (%) as shown in **Fig. 16 (a).** Based on this analysis, 40 layers of panels made with a 2D plain weave and 3D warp interlock p-aramid fabrics at the moulded target points possess 97.48% and 96.75% energy absorption respectively. Whereas the energy transmitted values beyond the 40 layer panel of 2D plain weave and 3D warp interlock p-aramid fabrics were recorded as 2.51% and 3.25% respectively. This primarily indicated that the energy absorbed by the 2D fabrics at the moulded target points shows 0.74% increment and 0.74 % decrement of energy absorption and transmitted energy values respectively compared to 3D warp interlock fabrics.

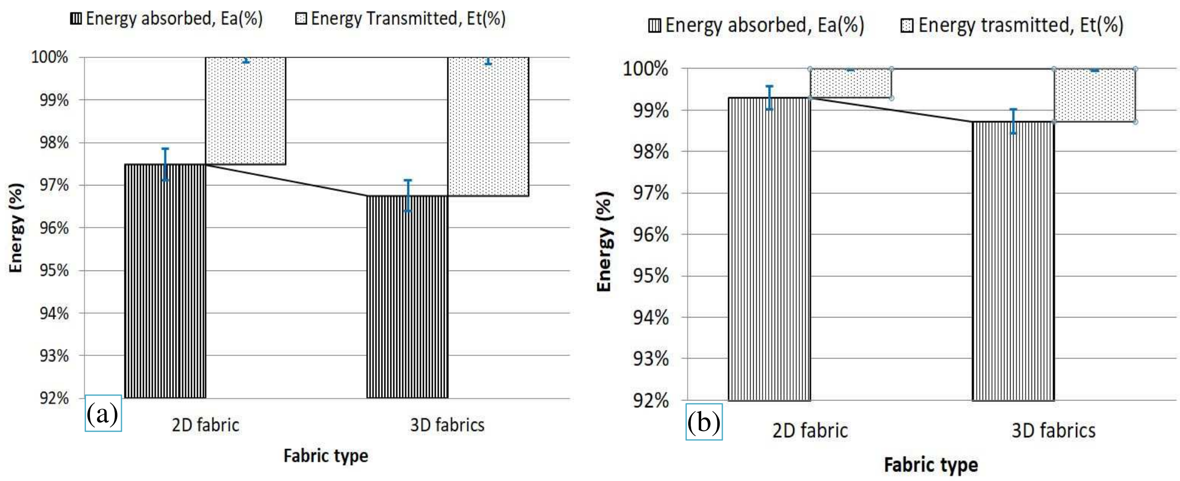

***Figure 16** Average energy absorption and transmission percentage of 2D plain and 3D warp interlock fabric of with 40 layers at (a) Moulded (d) area (average values of shot 1, 2 and 4) and (b) non-moulded (f) area (average values of shot 3, 5 and 6).*

In the other direction, the amount of absorbed and transmitted energy by the 2D plain weave and 3D warp interlock p-aramid fabrics considering the average values at the non-moulded (f) target points was analyzed. The average energy absorption and transmission percentage values for 40 layers of 2D plain weave and 3D warp interlock fabric panels at non-moulded (f) target area has been also discussed. For better analysis, other than the numerical values, it is also imperative to discuss more on the percentage values of the absorbed and transmitted energy both in the 2D plain weave and 3D warp interlock fabrics panel at non-moulded (f) target. Based on the ballistic test, the total ballistic impact energy exerted were found 659.79J and 664.71J on the 40 layers of 2D plain and 3D warp interlock fabrics panels at the non-moulded (f) target respectively. Among the total energy, 659.79J and 664.71J were recorded as average absorbed energy by the panels. However, 4.63J and 8.47J energy were transmitted beyond the intended panels of 2D plain weave and 3D warp interlock fabrics respectively. The percentage (%) values of the absorbed and transmitted energy by the intended panels (40 layers) of 2D plain weave and 3D warp interlock fabrics at non-moulded (f) target points were also highlighted as shown on **Fig. 16 (b).** Based on these investigations, their respective initial total impact energies, 99.29% and 98.72% were absorbed by the panels, whereas 0.7% and 1.27% of energy were transmitted beyond the panels of 2D plain weave and 3D warp interlock fabrics respectively. Unlike in the moulded target areas, the absorbed energy of the 2D plain weave panels show 0.67% of increment as compared to 3D warp interlocks panels. In the contrary, the energy transmitted to the backing material by the 2D plain panel's show 0.57% of decrement as compared to 3D warp interlock panels. This small difference does not show by itself as a significant effect in the energy absorbing capabilities of in the panels. 2D and 3D warp interlock fabrics with the same number of layers shows almost similar energy absorbing capabilities during ballistic impacts. Moreover, the conditions of target areas within the same number of fabrics type also show almost smaller difference both in energy absorption capabilities of the panel and its transmitted energy to the backing materials.

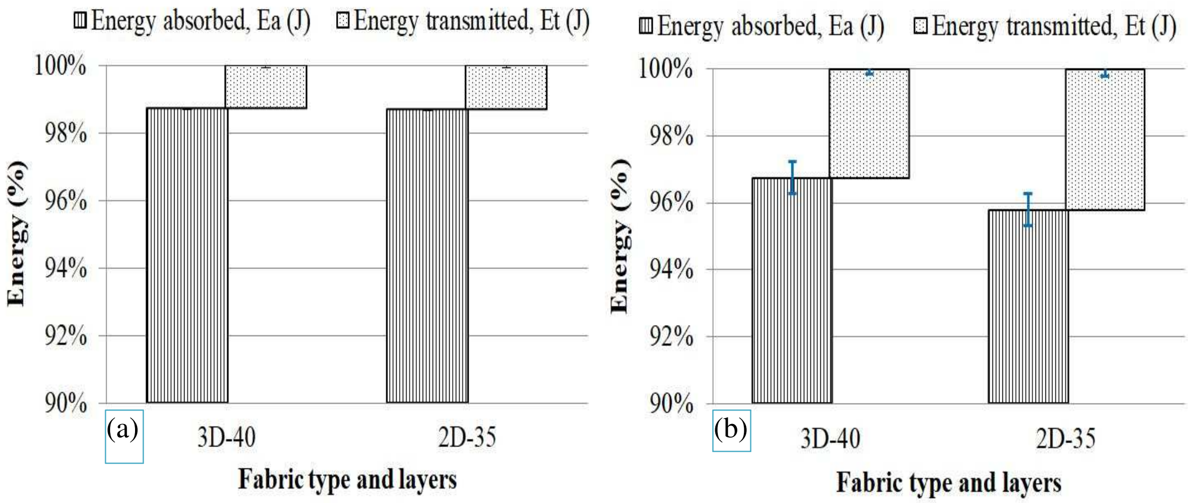

Figure 17. Average energy absorption and transmission values and its percentage of 2D plain weave and 3D warp interlock fabric with 35 and 40 layers respectively at (a) non-moulded (f) shooting area (average values of shot 3, 5 and 6) and (b) Moulded (d) shooting area (average values of shot 1 , 2 and 4).

As shown in **Fig. 17**, the average energy absorption and transmission values and its percentage of both 35 layers of 2D fabric and 40 layers of 3D fabric both at non-moulded (f) and moulded (d) target points were also investigated. The average percentage (%) energy absorbed and transmitted at the non-moulded (f) points of 35 layers of 2D fabrics panels was recorded as 98.68% and 1.31%. Whereas 98.7% and 1.27% values were observed in the non-moulded (f) points of target panels made with 40-layers 3D warp interlock fabric. On the contrary, the average percentage (%) energy absorbed and transmitted at the moulded (d) target points with 35 layers of 2D fabrics panels was recorded 95.8 % and 4.19%. A 96.75% and 3.25% values plotted for 40-layers of 3D warp interlock fabric panels in the moulded (d) target points. Besides, the average percentage of energy absorbed and transmitted while impacting 35 layers of 2D fabrics panel at deformed target area reveals almost similar values as for 40 layers of 3D fabrics panel compared to at the non-moulded points. As per the general observations, the energy absorption of 3D warp interlock fabric panel shows better capabilities in the moulded (d) target points than non-moulded (f) points as compared to 2D plain weave fabric panels. This indicated that 3D warp interlock fabrics in the moulded condition show better capabilities due to its extra mouldability without affecting the mechanical performances of the materials. However, the energy absorbed percentage panels made of 2D fabric possesses better values in the non-moulded (f) shot points as compared to the 3D warp interlock fabrics. This might be due to the stiffness property of 2D plain weave fabrics to give good ballistic protection abilities.

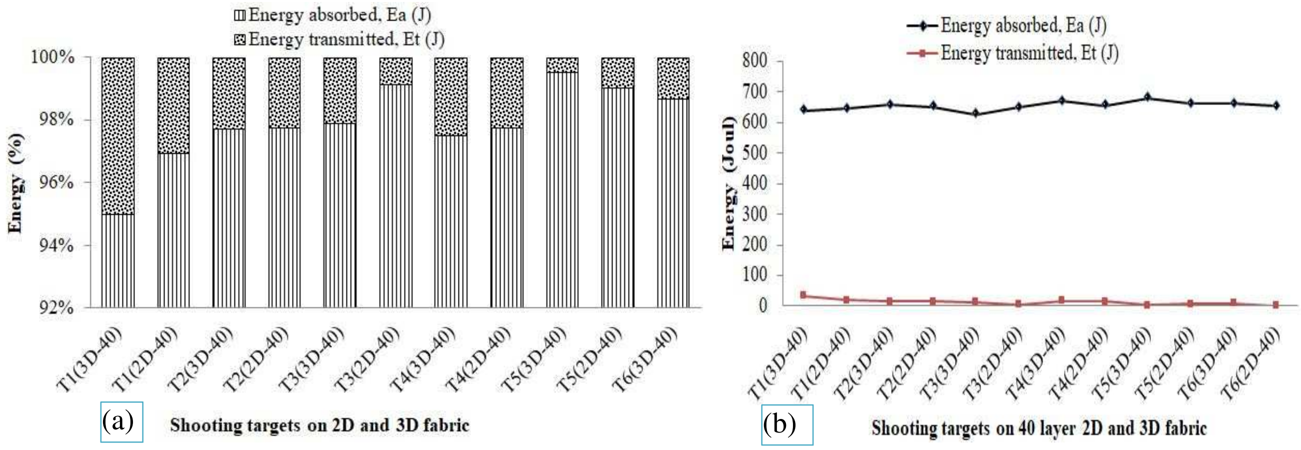

Figure 18 *Energy absorption and transmission values (Joule) and its percentage (%) of 2D plain weave and 3D warp interlock fabrics of both 40 layers at individual target shoot of non-moulded (f) area (T3, T5 and T6) and Moulded (d) area (T1, T2 and T4).*

Other than the average energy absorption and transmitted values (joule) and its percentage (%) values, each target areas for a predefined 40 layers 2D plain weave and 3D warp interlock fabrics were analyzed as shown in **Fig. 18.** Taking into account both types of fabric, the energy absorbed by the panel were found higher in the non-moulded (d) target points as compared to its counterpart corresponding moulded (d).areas. However, in a specific comparison between 2D plain weave and 3D warp interlock fabrics, the non-moulded (f) target points of 2D plain weave panel show better energy absorption capabilities in most points compared to 3D warp interlock fabrics. For example, non-moulded target area T1 (d) and T6 (f) show 1% and 1.1% higher energy absorption than the 3D warp interlock fabrics with similar target areas as shown in **Fig 18 (b)**. Similarly, the energy absorption capabilities of 2D plain weave fabric panel still show higher values in the moulded (d) target areas compared to the 3D warp interlock fabric panels. If we see the energy absorption capabilities of target areas as a whole, the values for moulded (d) target were found lower than the non-moulded target area for both types of fabric structure. The moulded (d) target area T1 (d), T2 (d) and T4 (d) had 94.98%, 97.74% and 97.52% for the 3D warp interlock fabric, whereas 96.93%, 97.74% and 97.76% of the 2D plain weave fabric. Similarly, the non-moulded (f) target area T3 (f), T5 (f) and T6 (f) revealed 97.9%, 99.54% and 98.69% for the 3Dwarp interlock fabrics and 99.14%, 99.03% and 99.73% for the 2D plain weave fabrics of energy absorption from the total impact energy.

3.2 Mouldability of 3D warp interlock and 2D plain p-aramid fabric structure

Mouldability is one of the important behaviours of material performance in the manufacturing of three-dimensional components. Mouldability of the textile structure is the capability of a flat textile material to be directly deformed to fit a three-dimensional surface without the formation of different defects including wrinkles, kinks or tears [48]. Besides, such process could increase both the productivity as well as the mechanical performances of the final product by maintaining the integrity within the material. Applying textile material with good mouldability could avoid cutting and assembling in the manufacturing of three-dimensional shape for different applications. Nowadays, various sectors including aerospace, military, vehicles etc. have used such manufacturing process to produce different components. For example, the most commonly used design approach for developing women soft body armour is a cut-and-sew method through dart application. However, the stitches used to create the dart line could create a weak area during the ballistic impact. Moulding method becomes an emerging designing method to form the women body armour by accommodating the bust without creating dart stich lines in order to eliminate the projectile impact weak point [49] [50] [44] [51][43]. However, in addition to its ballistic performance, the material should possess good moulding behavior in order to eliminate different defects including shear deformation thickness variations, and wrinkles while moulding.

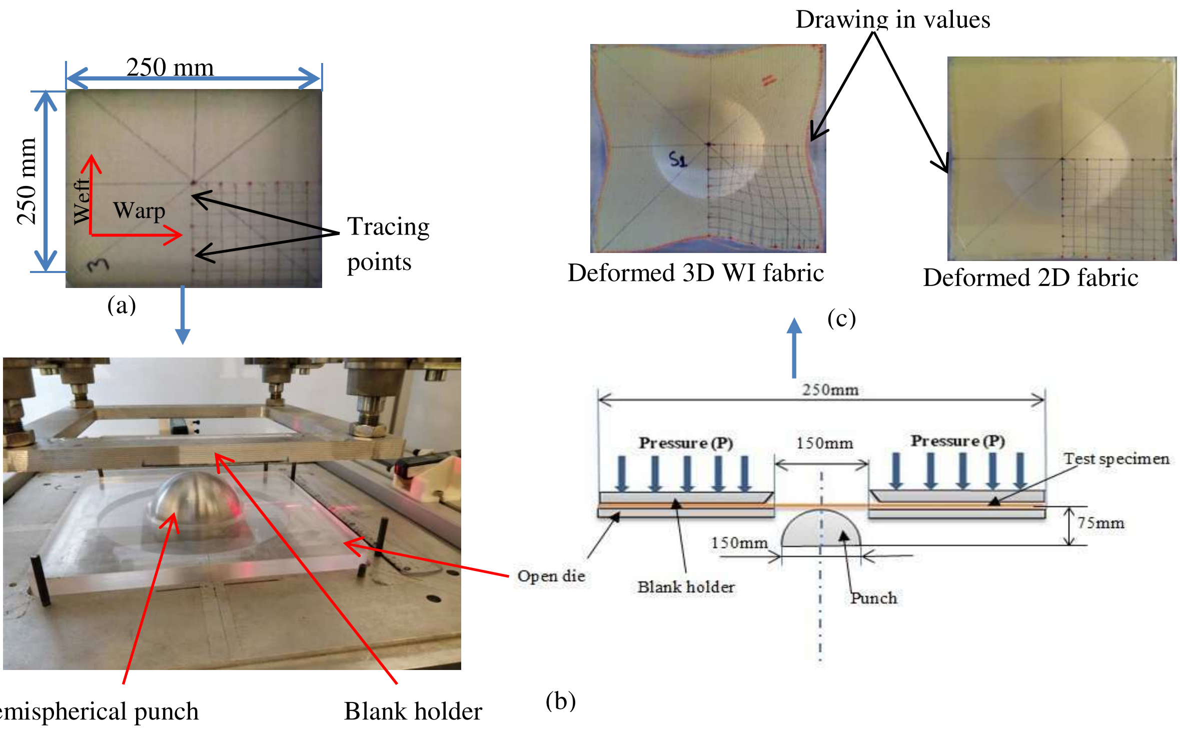

Figure 19 *Moulding test process of the fabrics (a) Prepared sample for moulding test, (b) hemispherical moulding bench and its set-up and (c) moulded 2D plain weave and 3D warp interlock specimens.*

Various researchers have mentioned that 3D angle interlock fabric structures should become a promising material for various applications including women body armour development due to its excellent moulding behaviours. One of our research works has also experimentally studied the different moulding behaviours of 3D warp interlocks and its counterpart 2D plain p-aramid fabrics made of similar p-aramid yarn [52]. For the study, the two fabrics with five layers of similar densities were prepared in squared 250 mm X 250 mm dimensions and tested using a modified pneumatic based forming bench as shown in **Fig. 19**. A predefined hemispherical punch with low stamping process was applied to mould the target with same parameters including blank holder pressure (**0.2MPa**), a velocity of the punch(**45 mm/s**), fabric and deforming depth (65 mm) [53]. Based on the result, the 2D fabric preform required high punching loads to deform the specific deformational depth as compared to 3D warp interlock fabrics preform. However, the 2D fabric faces lower drawing-in values with higher drawing-in recovery in all directions as compared to the corresponding 3D warp interlock fabrics. Moreover, according to the report, 2D plain weave fabric has also revealed higher values of recovery in the moulding depth directions as compared to its counterpart 3D warp interlocks fabrics. In general, these characteristics leave the 2D plain woven fabric in less mouldable fabric structure as compared to the 3D warp interlock fabrics with similar fabric densities.

Unlike the hemispherical punch; the current research has employed bust-shaped punch on the adapted forming bench (**Fig. 20(a)**). The results especially its recovery performances were similar to the hemispherical moulding process. The main purpose of using bust-shaped punch was to form the required women bust volumes and resemble frontal body armour shape. Unlike 3D warp interlock fabric panel, 2D plain weave fabric preform exhibited more wrinkles in its majority surfaces during the moulding process as shown in **Fig. 20 (b) and (c)**. The domed shapes of panels made of 2D fabrics have also shown a very fast deformational recovery in both dimensions and become flat very quickly. Whereas, the moulding recovery of the 3D warp interlock panels in all directions were insignificant for an extended period of time. Such stability behaviour after deformation with less surface damages makes the 3D warp interlock fabrics a good mouldable structure not only in the hemispherical punch but also in non-uniform punches including bust-shapes.

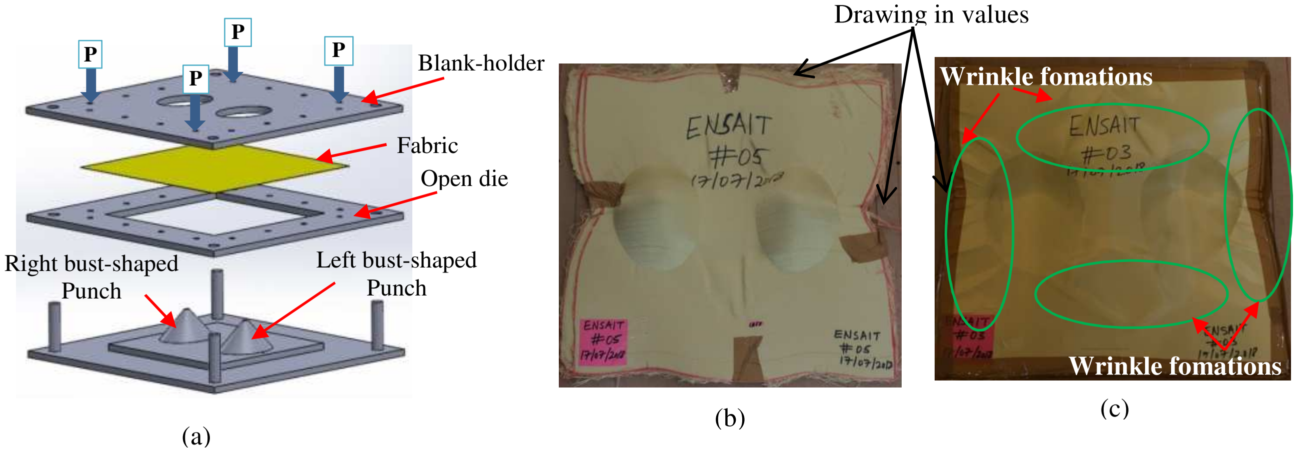

Figure 20 *Deformations of target panel to resemble the women frontal body shape (a) schematic view of adapted manual-based forming bench set up (b) deformed 3D warp interlock target panel and (c) deformed 3D warp interlock target panel.*

4. CONCLUSIONS

3D warp interlock and 2D plain weave p-aramid fabrics panels made of similar high-performance yarn (Twaron) were moulded to resemble the frontal female body shape and investigated against ballistic impact test according to NIJ-Level IIIA for female body armour solution. The measured trauma volumes for each target impact were used to determine the amount of absorbed energy by the panels. Based on the result, the ballistic protection capabilities of 3D warp interlock fabric show no significant difference as compared to 2D plain woven fabrics with similar fabric density while using higher number of layers. However, due to its structural compactness and rigidity, 2D plain p-aramid woven fabrics possess good ballistic performance with the minimum number of layers as compared to 3D warp interlock fabrics. For example, 40-layers of 2D plain weave and its corresponding 3D warp interlock fabrics panels' shows similar deformation and energy absorption capability. However, 30 layer of 2D plain fabric has still shown good ballistic performance as compared to its counterpart 3D warp interlock fabric. Moreover, even though it is not much significant, the energy absorption capabilities of the panel at the non-moulded target area have also revealed better values than the moulded target areas. This is due to the fact that, while moulding the panel, the compactness and rigidity of the panel in the specified area has been compromised and ultimately gives lower mechanical and ballistic performances. On contrary, 3D warp interlock fabric show better shaping ability according to the female contour while designing the body armour than its counterpart 2D plain weave p-aramid fabric. Finally, since fabrics type along with rigidity property were found a significant factor for designing women seamless female body armour, further studies are planned to work on model simulation followed by experimental validation on proper designing of 3D warp interlock fabric structure with more stiff, rigidity and compactness to acquire higher impact resistance without compromising its moulding behaviour.

5. COMPLIANCE WITH ETHICAL STANDARD

We declare there is no any financial or/and relevant interest that will influence the study. The study also consents for any involvement in the study.

6. ACKNOWLEDGEMENT

This work has been done as part of Erasmus Mundus Joint Doctorate Programme SMDTex-sustainable Management and Design for Textile project, which is financially supported by the European Erasmus Mundus Program. Moreover, the authors would like to thank 'Centre de Recherche et d'Expertise de La Logistique (CREL)' ballistic impact test facilities located in Paris, France and its crew members for providing the ballistic facilities and to their help while testing the samples. Authors would like also to thank M François Dassonville for his help during the ballistic tests and scanning of Blunt trauma deformation in the backing material.

7. REFERENCES

[1] M. El Messiry and S. El-tarfawy, “Performance of Weave Structure Multi-Layer Bulletproof Flexible Armor,” in *The 3rd conference of the National Campaign for Textile Industries,NRC Cairo, “‘Recent Manufacturing Technologies and Human and Administrative Development,’”* 2015, pp. 218–225.

[2] A. R. Othman and M. H. Hassan, “Effect of different construction designs of aramid fabric on the ballistic performances,” *Mater. Des.*, vol. 44, pp. 407–417, 2013.

[3] P. M. Cunniff, “An Analysis of the System Effects in Woven Fabrics Under Ballistic Impact,” *Text. Res. J.*, vol. 62, no. 9, pp. 495–509, 1992.

[4] D. Sun, X. Chen, and G. Wells, “Engineering and analysis of gripping fabrics for improved ballistic performance,” *J. Compos. Mater.*, vol. 0, no. 0, pp. 1–10, 2013.

[5] R. Yadav, M. Naebe, X. Wang, and B. Kandasubramanian, “Body armour materials: from steel to contemporary biomimetic systems,” *RSC Adv.*, vol. 6, no. 116, pp. 115145–115174, 2016.

[6] M. Karahan, A. Jabbar, and N. Karahan, “Ballistic impact behavior of the aramid and ultra-high molecular weight polyethylene composites,” *J. Reinf. Plast. Compos.*, vol. 34, no. 1, pp. 37–48, 2015.

[7] B. A. Cheeseman and T. A. Bogetti, “Ballistic impact into fabric and compliant composite laminates,” *Compos. Struct.*, vol. 35, no. 18, pp. 161–173, 2003.

[8] P. Bajaj, “Ballistic protective clothing : An overview,” *Indian J. Fibre Text. Res.*, vol. 22, no. 4, pp. 274–291, 1997.

[9] A. Bhatnagar, B. Arvidson, and W. Pataki, *Lightweight Ballistic Composites, Military and Law-Enforcement Applications*. Woodhead Publishing, 2006, p. 213-214, 2006.

[10] C. R. Cork and P. W. Foster, “The ballistic performance of narrow fabrics,” *Int. J. Impact Eng.*, vol. 34, pp. 495–508, 2007.

[11] M. O. Yavaşa, A. Avcıa, M. Şimşirb, and A. Akdemira, “Ballistic performance of Kevlar49/ UHMW-PEHB26 Hybrid Layered- Composite,” *Int. J. Eng. Res. Dev.*, vol. 7, no. 4, pp. 1–20, 2015.

[12] J. L. Park, Y. Chi, and T. J. Kang, “Ballistic performance of hybrid panels composed of unidirectional/woven fabrics,” *Text. Res. J.*, vol. 83, no. 5, pp. 471–486, 2013.

[13] Y. Wang, X. Chen, R. Young, I. Kinloch, and G. Wells, “An Experimental study of ply orientation on ballistic impact resistance of multi-ply fabric panels,” *Compos. Part B Eng.*, vol. 68, pp. 259–265, 2015.

[14] B. J. Briscoe and F. Motamedi, “The ballistic impact characteristics of aramid fabrics: The influence of interface friction,” *Wear*, vol. 158, pp. 229–247, 1992.

[15] V. B. C. Tan, T. E. Tay, and W. K. Teo, “Strengthening fabric armour with silica colloidal suspensions,” *Int. J. Solids Struct.*, vol. 42, pp. 1561–1576, 2005.

[16] M. Karahan, “Comparison of Ballistic Performance and Energy Absorption Capabilities of Woven and Unidirectional Aramid Fabrics,” *Text. Res. J.*, vol. 78, no. 8, pp. 718–730, 2016.

[17] S. B. Brantner, “policeone.com,” *Police History: The evolution of women in American law enforcement*, 2015. [Online]. Available: https://www.policeone.com/police-history/articles/8634189-Police-History-The-evolution-of-women-in-American-law-enforcement/. [Accessed: 23-Dec-2016].

[18] S. Das, S. Jagan, A. Shaw, and A. Pal, “Determination of inter-yarn friction and its effect on ballistic response of para-aramid woven fabric under low velocity impact,” *Compos. Struct.*, vol. 120, pp. 129–140, 2015.

[19] C. C. Yang, T. Ngo, and P. Tran, “Influences of weaving architectures on the impact resistance of multi-layer fabrics,” *Mater. Des.*, vol. 85, pp. 282–295, 2015.

[20] M. Karahan, “Comparison of Ballistic Performance and Energy Absorption Capabilities of Woven and Unidirectional Aramid Fabrics,” *Text. Res. J.*, vol. 78, no. 8, pp. 718–730, 2008.

[21] D. Zhang, Y. Sun, L. Chen, S. Zhang, and N. Pan, “Influence of fabric structure and thickness on the ballistic impact behavior of Ultrahigh molecular weight polyethylene composite laminate,” *Mater. Des.*, vol. 54, pp. 315–322, 2014.

[22] A. K. Bandaru, L. Vetiyatil, and S. Ahmad, “The effect of hybridization on the ballistic impact behavior of hybrid composite armors,” *Compos. Part B Eng.*, vol. 76, pp. 300–319, 2015.

[23] L. H. Nguyen, S. Ryan, S. J. Cimpoeru, A. P. Mouritz, and A. C. Orifici, “The effect of target thickness on the ballistic performance of ultra high molecular weight polyethylene composite,” *Int. J. Impact Eng.*, vol. 75, pp. 174–183, 2015.

[24] M. P. Rao, Y. Duan, M. Keefe, B. M. Powers, and T. A. Bogetti, “Modeling the effects of yarn material properties and friction on the ballistic impact of a plain-weave fabric,” *Compos. Struct.*, vol. 89, no. 4, pp. 556–566, 2009.

[25] T. L. Chu, C. Ha-Minh, and A. Imad, “A numerical investigation of the influence of yarn mechanical and physical properties on the ballistic impact behavior of a Kevlar KM2®woven fabric,” *Compos. Part B Eng.*, vol. 95, pp. 144–154, 2016.

[26] Y. Duan, M. Keefe, T. A. Bogetti, B. A. Cheeseman, and B. Powers, “A numerical investigation of the influence of friction on energy absorption by a high-strength fabric subjected to ballistic impact,” *Int. J.*

Impact Eng., vol. 32, no. 8, pp. 1299–1312, 2006.
[27] M. Karahan, A. Kuş, and R. Eren, "An investigation into ballistic performance and energy absorption capabilities of woven aramid fabrics," *Int. J. Impact Eng.*, vol. 35, no. 6, pp. 499–510, 2008.
[28] H. S. Learmont, "Soft armor," patent number US 7,251,835 B2, 2007.
[29] Pa. Purushothaman, G. Coimbatore, and S. S. Ramkumar, "Soft Body Armor for Law Enforcement Applications," *J. Eng. Fiber. Fabr.*, vol. 8, no. 2, pp. 97–103, 2013.
[30] X. Chen, D. Sun, Y. Wang, and Y. Zhou, "2D / 3D Woven Fabrics for Ballistic Protection," in *4th World Conference on 3D Fabrics and Their Applications ; 10 Sep 2012-11 Sep 2012; Aachen, Germany. Manchester: TexEng/RWTH Aachen*, 2012, pp. 1–12.
[31] M. Lefebvre and F. Boussu, "High energy absorption of warp interlock fabrics : Application to high speed impact of fragments," in *DYMAT International Conferences*, 2009, no. DYMAT 2009 (2009), pp. 429–435.
[32] F. Boussu, X. Legrand, S. Nauman, and C. Binetruy, "Mouldability of angle interlock fabrics," in *in FCPM , the 9th International Conference on Flow Processes in Composite Materials*, 2008, vol. 9, no. July.
[33] K. Bilisik, "Two-dimensional (2D) fabrics and three-dimensional (3D) preforms for ballistic and stabbing protection: A review," *Text. Res. J.*, vol. 0, no. 00, pp. 1–30, 2016.
[34] D. Sun and X. Chen, "Three-dimensional textiles for protective clothing," in *Advances in 3D Textiles*, 2015, pp. 341–360.
[35] J. H. Byun and T. W. Chou, "Elastic Properties of Three- dimensional Angle-interlock Fabric Preforms," *J. Text.*, vol. 81, no. 4, pp. 538–548, 1990.
[36] Xiaogang Chen and Dan Yang, "Use of 3D Angle-Interlock Woven Fabric for Seamless Female Body Armour : Part I :Ballistic Evaluation," *Text. Res. J.*, vol. (0), no. (0), pp. 1–8, 2010.
[37] X. Chen, W.-Y. Lo, and A. E. Tayyar, "Mouldability of Angle-Interlock Woven Fabrics for Technical Applications," *Text. Res. J.*, vol. 72, no. (3), pp. 195–200, 2002.
[38] C. Ha-Minh, A. Imad, F. Boussu, and T. Kanit, "Experimental and numerical investigation of a 3D woven fabric subjected to a ballistic impact," *Int. J. Impact Eng.*, vol. 88, pp. 91–101, 2016.
[39] M. Lefebvre, F. Boussu, and D. Coutellier, "Influence of warp interlock parameters on the ballistic behavior of a structure," *Proc. 10th Int. Conf. Text. Compos. - TEXCOMP 10 Recent Adv. Text. Compos.*, no. October, pp. 322–328, 2010.
[40] D. Yang *et al.*, "Ballistic performance of angle-interlock woven fabrics," *J. Text. Inst.*, vol. 108, no. 4, pp. 586–596, 2017.
[41] M. A. Abtew, P. Bruniaux, and F. Boussu, "Development of adaptive bust for female soft body armour using three dimensional (3D) warp interlock fabrics: Three dimensional (3D) design process," *IOP Conf. Ser. Mater. Sci. Eng.*, vol. 254, no. 5, p. 052001, 2017.
[42] M. A. Abtew, P. Bruniaux, F. Boussu, C. Loghin, I. Cristian, and Y. Chen, "Development of comfortable and well-fitted bra pattern for customized female soft body armor through 3D design process of adaptive bust on virtual mannequin," *Comput. Ind.*, vol. 100, no. 2018, pp. 7–20, 2018.
[43] M. A. Abtew *et al.*, "Female seamless soft body armor pattern design system with innovative reverse engineering approaches," *Int. J. Adv. Manuf. Technol.*, vol. 98, pp. 2271–2285, 2018.
[44] M. A. Abtew *et al.*, "A systematic pattern generation system for manufacturing customized seamless multi-layer female soft body armour through dome-formation (moulding) techniques using 3D warp interlock fabrics," *J. Manuf. Syst.*, vol. 49, no. June, pp. 61–74, 2018.
[45] M. B. Mukasey, J. L. Sedgwick, and D. W. Hagy, "Ballistic Resistance of Body Armor NIJ Standard-0101.06,Office of Science and Technology, National Institute of Justice, Washington, DC, NIJ Standard–0101.06 NCJ 223054," 2008.
[46] "U.S. Department of Justice, ballistic Resistance of Body Armor, NIJ Standard-0101.06.," *Law Enforc. Correct. Stand. Test. Progr.*, pp. 1–67, 2000.
[47] R. Prather, C. Swann, and C. Hawkins, "Backface Signatures of Soft Body Armors and the Associated Trauma Effects," 1977.
[48] T. Zhong and H. Hu, "Formability of weft-knitted fabrics on a hemisphere," *Autex Res. J.*, vol. 7, no. 4, pp. 245–251, 2007.
[49] X. Chen and D. Yang, "Use of 3D Angle-Interlock Woven Fabric for Seamless Female Body Armour: Part 1: Ballistic Evaluation," *Text. Res. J.*, vol. 0, no. 0, pp. 1–8, 2010.
[50] X. Chen and D. Yang, "Use of Three-dimensional Angle-interlock Woven Fabric for Seamless Female Body Armor : Part II : Mathematical Modeling," *Text. Res. J.*, vol. Vol 80, no. 15, pp. 1589–1601, 2010.
[51] D. Yang and X. Chen, "Multi-layer pattern creation for seamless front female body armor panel using angle-interlock woven fabrics," *Text. Res. J.*, vol. 0, no. 00, pp. 1–6, 2017.
[52] M. A. Abtew *et al.*, "Influences of fabric density on mechanical and moulding behaviours of 3D warp interlock para-aramid fabrics for soft body armour application," *Compos. Struct.*, vol. 204, no. April, pp. 402–418, 2018.

[53] C. Dufour, F. Boussu, P. Wang, and D. Soulat, “Experimental Forming Studies on 3D Warp Interlock Fabrics,” *Eccm16 - 16Th Eur. Conf. Compos. Mater.*, no. September 2016, 2014.

Appendix I **NIJ standard – 0101.06 P – BFS performance test summary**

Armour type	**Test Round**	**Test Bullet**	**Bullet Mass**	**Conditioned Armour Test Velocity(m/s)**	**Hit per panel at 0° angle**	**Maximum BFS depth**	**Hits per panel at 30° or 40°**	**Shot per Panel**	**Panel Required**	**Shot Required**	**Total Shots required**
IIA	1	9 mm FMJ RN	8.0 g (124gr)	355 m/s (1165 ft/s)	4	44 mm (1.73 in)	2	6	4(LN) 2(LC) & 4(SN) 2(SC)	24(LN) 12 (LC) & 24(SN) 12(SC)	144
	2	40 S&W FMJ	11.7 g (180 gr)	325 m/s (1066 ft/s)	4	44 mm (1.73 in)	2	6	4(LN) 2(LC) & 4(SN) 2(SC)	24(LN) 12 (LC) & 24(SN) 12(SC)	144
II	1	9 mm FMJ RN	8.0 g (124gr)	379 m/s (1245 ft/s)	4	44 mm (1.73 in)	2	6	4(LN) 2(LC) & 4(SN) 2(SC)	24(LN) 12 (LC) & 24(SN) 12(SC)	144
	2	.357 Mag JSP	10.2 g (158gr)	408 m/s (1340 ft/s)	4	44 mm (1.73 in)	2	6	4(LN) 2(LC) & 4(SN) 2(SC)	24(LN) 12 (LC) & 24(SN) 12(SC)	144
IIIA	1	.357 SIG FMJ FN	8.1 g (125gr)	430 m/s (1410 ft/s)	4	44 mm (1.73 in)	2	6	4(LN) 2(LC) & 4(SN) 2(SC)	24(LN) 12 (LC) & 24(SN) 12(SC)	144
	2	.44 Magnum SJHP	15.6 g (240gr)	408 m/s (1340 ft/s)	4	44 mm (1.73 in)	2	6	4(LN) 2(LC) & 4(SN) 2(SC)	24(LN) 12 (LC) & 24(SN) 12(SC)	144
III	1	7.62 mm NATO FMJ	9.6 g (147gr)	847 m/s (2780 ft/s)	**6**	44 mm (1.73 in)	2	6	4 (all conditioned)	24	24
IV	1	.30 Caliber M2 AP	10.8 g (166gr)	878 m/s (2880 ft/s)	**1 to 6**	44 mm (1.73 in)	2	6	4-24 (all conditioned)	24	24
Special		Each threats to be specified by manufacturers or Procuring organizations			Armour performance and shot requirement depends on the armour type						

* LN and LC stands for a large size with new panels and large size with conditioned panel respectively
* SN and SC stands for Small size with new panels and Small size with conditioned panel respectively

8. Figure Captions

Figure 1 *3D warp interlock production process (a) design schematic representation in a cross section (TexGen software); (b) 3D graphical representation (TexGen software); (c) 3D warp interlock fabric production on loom and (d) and (e) Top and side view of the produced 3D warp interlock fabric respectivly.*

Figure 2 *2D plain weave para-aramid fabric structures, Twaron CT-709 (a) Design schematic representation, and (b) 2D plain weave fabrics.*

Figure 3*. Moulded sample target preparation (a) Moulding of target panels on adapted moulding bench, (b) Target panel before moulding, and (d) Moulded sample target panel.*

Figure 4 *Ballistic testing set-up and backing material (a) Ballistic test apparatus, (b) gun barrel and bullet used, (c) Square box filled with backing clay material and bust-shaped* *moulded clay, and (d) panel target with shooting point.*

Figure 5 *Blunt trauma measurement process (a) Panels for the ballistic test (b) Blunt trauma indentation after shooting, (c) All the trauma indentation and, ((d) Scanning of backing material after the test using the handy scanner for trauma measurement.*

Figure 6 *Scanned backing material after ballistic test and its trauma indentations of different panel targets (a) 2D plain weave and (b) 3D warp interlock fabrics.*

Figure 7 *Determinations of trauma volumes for different target shot using 3D design software (a) Modelled 3D backing material surface with different shot trauma (b) Creation of internal and outer framework following the trauma indentation (c) Modelling of out and inner surface mesh trauma volume (d) Stitched out and inner surface to develop blunt trauma volume.*

Figure 8 *Calibrations of clay backing material.*

Figure 9 *Ballistic results of 40 layers of 2D plain weave fabric at different shooting areas (moulded (d) and non-moulded (f) area) (b) Values of absorbed and transmitted energy in Joule and (b) Percentages (%) of absorbed and transmitted energy.*

Figure 10 *Ballistic results of 35 layers of 2D plain weave fabric at different shooting areas (moulded (d) and non-moulded (f) area) (a) Values of absorbed and transmitted energy in Joule and (b) Percentages (%) of absorbed and transmitted energy.*

Figure 11 *Ballistic results of 30 layers of 2D plain fabric at different shooting areas (moulded (d) and non-moulded (f)) (a) Values of absorbed and transmitted energy in Joule and (b) Percentages (%) of absorbed and transmitted energy.*

Figure 12 *Ballistic results of 40 layers of 3D warp interlock fabric at different shooting areas (moulded (f) and non-moulded (f) area) (a) Values of absorbed and transmitted energy in Joule and (b) Percentages (%) of absorbed and transmitted energy.*

Figure 13 *Ballistic results of 30 layers of 3D warp interlock fabric at different shooting areas (moulded (d) and non-moulded (f) area) (a) Values of absorbed and transmitted energy in Joule and (b) Percentages (%) of absorbed and transmitted energy.*

Figure 14 *Average energy absorption and transmission and its percentage of 2D fabric with different layers at non-moulded (f) area (shot 3, 5 and 6).*

Figure 15 *Average energy absorption and transmission and its percentage of 2D fabric with different layers at moulded (d) area (shot 1, 2 and 4).*

Figure 16 *Average energy absorption and transmission percentage of 2D plain and 3D warp interlock fabric of with 40 layers at (a) Moulded (d) area (average values of shot 1, 2 and 4) and (b) non-moulded (f) area (average values of shot 3, 5 and 6).*

Figure 17*. Average energy absorption and transmission values and its percentage of 2D*

plain weave and 3D warp interlock fabric with 35 and 40 layers respectively at (a) non-moulded (f) shooting area (average values of shot 3, 5 and 6) and (b) Moulded (d) shooting area (average values of shot 1 , 2 and 4).

Figure 18 *Energy absorption and transmission values (Joule) and its percentage (%) of 2D plain weave and 3D warp interlock fabrics of both 40 layers at individual target shoot of non-moulded (f) area (T3, T5 and T6) and Moulded (d) area (T1, T2 and T4).*

Figure 19 *Moulding test process of the fabrics (a) Prepared sample for moulding test, (b) hemispherical moulding bench and its set-up and (c) moulded 2D plain weave and 3D warp interlock specimens.*

Figure 20 *Deformations of target panel to resemble the women frontal body shape (a) schematic view of adapted manual-based forming bench set up (b) deformed 3D warp interlock target panel and (c) deformed 3D warp interlock target panel.*